Geodynamics and Space Geodesy

The "Geo" sciences in the Laboratory of Terrestrial Physics largely reside in the Geodynamics Branch and the Space Geodesy Branch. Together these groups study a wide range of subjects in the broad disciplines of geophysics, geology, geodesy and geodynamics for both the Earth and solid planetary bodies, especially Mars. Present-day measurements using both surface and satellite data, models derived from these, and other observational and theoretical information are used to help improve our understanding of the evolution of the core, mantle and crust, and their interactions with the fluid envelopes at and above the surface. Major areas of work are described in more detail below, and examples of major accomplishments in the last year are provided in the following sections.

Geodynamics includes studies of the surface and interior of the Earth and planets: their current state, including dynamics, and the processes which operate to produce the observed state and motions. Specific areas of research and study include the following:

(1) Core fluid motions and how it relates to changes in the Earth's magnetic field;

(2) Motions of the Earth's crust and the relationship with earthquake hazard, especially in areas of active subduction;

(3) Vertical rebound of paleolakes and the constraints it provides on lower crustal and upper mantle properties;

(4) Long term orbital-rotational evolution and its relationship to long term climate change;

(5) Magnetic properties of the Earth's crust and the nature of the sources of magnetic anomalies not just on the Earth but on Mars as well;

(6) Topographic characterization of the surface of the Earth and Mars, in the former case to understand landforms associated with active faulting, in the latter case to understand volcanic and tectonic structures and the origin of the fundamental crustal topographic dichotomy, and how large scale impacts affect early crustal evolution.

Space geodesy involves positional studies of the Earth's surface and its orientation in space, the Earth's gravity field, and the use of their time evolution to understand fundamental Earth processes. The latter include mantle convection, plate motion, and fluid mass transports both on the surface (e.g., ocean and atmospheric circulation, land hydrology, icesheets) and in the core. Active areas of work incorporate the following:

(1) Determination of the precise orbits for Earth satellites and planetary spacecraft and determination of the Earth's fundamental reference frame;

(2) Gravity field model development for Earth and other planets, both the static and time-varying components;

(3) Oceanic and solid body tidal processes and the resultant deformation of the Earth;

(4) The effects of redistribution of geophysical fluids (air, water, ice) on the Earth and their manifestation in, for example, the time-variable gravity field and Earth rotation parameters;

(5) Analysis and modeling of space-geodetic Very-Long-Baseline Interferomettry measurements and applications to Earth's rotation studies: and

(6) Development of space techniques that enable precise measurement of the above- mentioned geodetic observables.

Brief descriptions of each of the major areas of work are provided below. Individual significant highlights of the past year are provided, along with contact information for the relevant author.

Background for each of these areas can be found in the 2001 Annual Report. Additional progress and ongoing work for this year is indicated by papers given at national and international meetings during the year.

Geomagnetism

Understanding Geomagnetic Field Variation with Numerical Modeling

Surface and space geomagnetic observations identify that the Earth's magnetic environment varies on a wide spectrum of time scales, from seconds to millions of years. While external sources (e.g. electromagnetic processes in ionsphere and magneosphere) contributes to small and fast varying disturbances near the Earth's surface, the most significant changes arise from the dynamical processes in the Earth's liquid outer core. The outer core is in vigorous convection, driven by gravitational energy released from secular cooling of the Earth. This turbulent convection generates and maintains a strong core field (accounting for 97% of the total magnetic energy observed at the surface of the Earth) that varies on time scales up to millions of years.

The Modular, Scalable, Self-consistent, Three-dimensional (MoSST) numerical model, under constant development in our Laboratory, is able to explain qualitatively the physics of the geomagnetic field generation (geodynamo), and to model possible force balances in the core, such as the Taylor's constraint that governs torsional oscillations on decadal time scales. Advances in this model, together with new geomagnetic observations (from e.g. Ørsted, Champ, Ørsted-2/SAC-C),are making feasible the assimilation of observational data to numerical dynamo simulation. With this research, it could be able to predict long-time geomagnetic secular variation, and to constrain numerical core dynamics modeling via observational results.

In 2002, a new algorithm was introduced to the model that could reduce Computing Processor Unit (CPU) time by one order of magnitude, greatly speeding up the simulation process. The initial testing confirmed the expectation. Further testing and benchmarking are in process prior to fully implementing the algorithm. In addition, activities were advanced on geomagnetic data assimilation. Researchers from Code 921, Code 926 and Data Assimilation Office (DAO) are examining the discrepancies between the MoSST dynamo results, observed geomagnetic field (derived from NASA Comprehensive model that utilizes surface and satellite data from Magsat, Ørsted and Champ, and appropriate assimilation algorithms to produce analysis states for assimilation. These initial results are very encouraging: while there is no correlation between the two results in the absence of any data assimilation, it was found that with a very crude (non-optimized) data insertion (to the modeling results), certain correlation is shown between the two results, as shown in Figure 1.

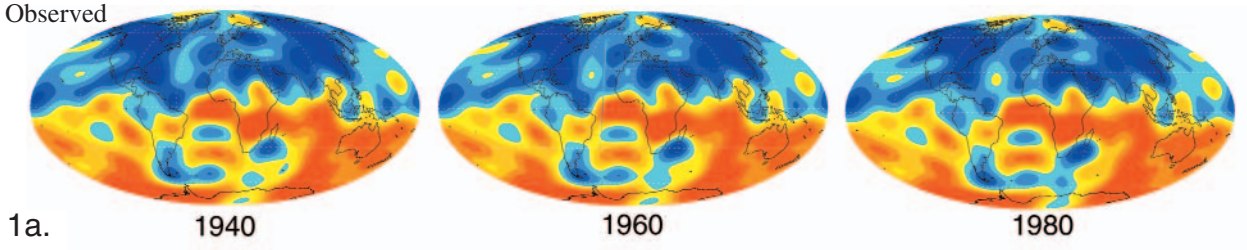

1a.

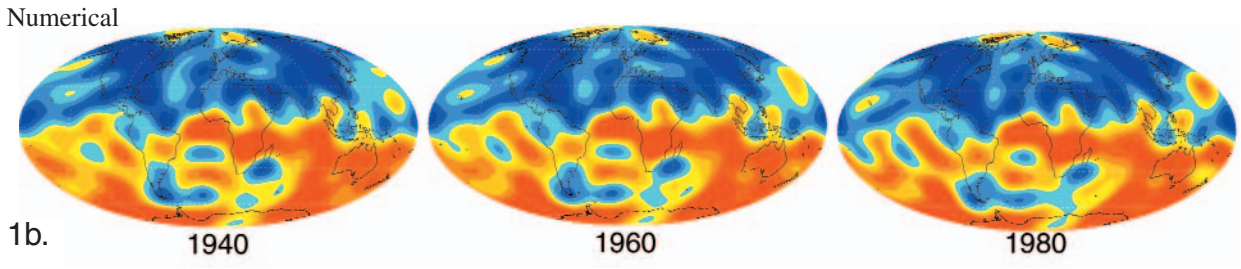

Figure 1. Examples of geomagnetic data assimilation. 1a, (see bottom of previous page) is three snapshots of the observed geomagnetic field morphology at the core-mantle boundary (CMB). 1b (above) is the results from MoSST numerical modeling, in which the analysis state (initial solution) is obtained by inserting the observed field in 1940 to a numerical dynamo solution. The assimilated results are similar to observations, in particular the large-scale features, such as the south Atlantic anomaly.

Contact: Contact: Weijia Kuang, Weijia.Kuang-1@nasa.gov

Comprehensive Field Modeling Paper Published

Ongoing improvements in the development of the GSFC Comprehensive Model reached a milestone with the recent publication of a major paper by Sabaka et al. (2002). This model, based on data from POGO, Magsat, and ground-based observations, represents the state-of-the-art in main field models, and includes parameterized components for the external fields and the lithospheric fields as well as the core field. This same year has seen further refinements in comprehensive modeling (CM) efforts, led by Terry Sabaka, which were reported on at the 4th Ørsted International Science Team meeting in Copenhagen, Denmark in September (see below). The latest improvements include additional data from the most recent magnetic mapping missions, the Danish Ørsted and German CHAllenging Mini-Satellite Payload (CHAMP) satellites. These push the model envelope from an earlier 1960-1985 to a period covering 1960-mid 2002. In addition to extension of the main field secular variation model, a much lower noise lithospheric field was derived (Figure 2). In-situ currents through which Ørsted flies are now modeled in continuous diurnal time.

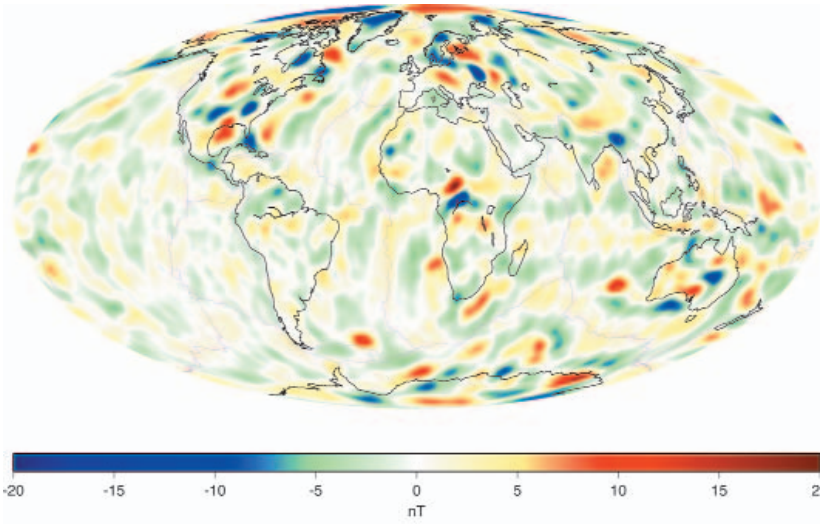

Figure 2. Lithospheric anomalies from the latest Comprehensive Model, including Ørsted and CHAMP data. These have much less noise than in earlier models.

Goddard's comprehensive models are now being used for a variety of applications. For example, the model will be used as the basis for removal of contamination from long-wavelength and diurnal variations in the planned USGS High Altitude Magnetic Mapping (HAMM) mission (an aeromagnetic survey). They have also been used by several research groups and in industry. Current and future programs using the Comprehensive Models include multi-satellite in-flight calibration efforts (Olsen et al., 2002) and mission simulation studies for the proposed SWARM (constellation) mission. Because of the increasing demand for these models, a website is being developed that will offer the latest models, codes and documentation. As part of this outreach effort, Sabaka has developed a versatile forward code available in ANSI Fortran, which computes magnetic and electric current density fields at positions in space and time, and also returns model coefficients in various forms.

References:

Olsen, N., L. Toffner-Clausen, T. Risbo, P. Brauer, J. Merayo, F. Primdahl and T. Sabaka, In-flight calibration methods used for the Ørsted mission, Earth Planets and Space, 2002 (accepted).

Sabaka, T.J., N. Olsen and R.A. Langel, A comprehensive model of the quiet-time, near-Earth magnetic field: phase 3, Geophys. J. Int., 151, 32-68, 2002.

Contact: Terry Sabaka, Sabaka@geomag.gsfc.nasa.gov

American Geophysical Union (AGU) Virtual Session Held

In what may be a template for the future, AGU conducted a "virtual session" during its Spring Meeting, using a web-based protocol to bring together participants from around the world. Mike Purucker was one of the chief organizers of session GP21A, which discussed analysis of selected, previously posted, data from the "mini-constellation" of magnetic field satellites Ørsted, CHAMP and SAC-C. 27 authors and co-authors from nine different countries were involved.

Figure 3. Michael Purucker and 26 other authors from nine countries engaged in a "virtual" session as part of the Spring 2002 AGU Meeting.

One of the main topics discussed was the apparently forced decay of the Earth's dipolar field, which is occurring 10 times faster than would happen if the core dynamo (which generates the field) were suddenly switched off. Growing patches of reversed polarity field are believed responsible. If these continue to grow they could lead to a new reversal of the Earth's field as has occurred in the past.

In preparation for this unique event, 19 days of common satellite data were selected and posted on a dedicated web site, in order that different analysis methods could be applied to the same data. The community was alerted to the virtual session through e-mail with a link provided to the web site. The data became available in January and February, and abstracts submitted and posted in March. Authors submitted their presentations in early May which were made available on the web site. The "live" session was actually held in 2-hour periods on May 28th and 29th.

Following the actual "live" session, discussions were appended in June and a CD with papers and data was distributed to the authors. This follow-up is another unique aspect of the virtual session method of holding international meetings. A meeting report appeared in the August 20 issue of EOS (v.83, p. 368, 2002) in the "About AGU" section.

Contact: Mike Purucker, purucker@geomag.gsfc.nasa.gov

SWARM Constellation Selected by ESA

In May of 2002, the European Space Agency (ESA) selected three new Earth Opportunity Mission candidates for possible launch in the 2007-2009 time frame. One of those missions, SWARM, is a multi-satellite mission designed to study the multitude of magnetic fields encountered in near-Earth space. Mike Purucker is one of several U.S. co-investigators (3 are from GSFC!) on the SWARM science team, and is the only U.S. participant asked by ESA to serve on the Mission Advisory Group (MAG) during the 1.5 year Phase A Study period. At the end of this time a decision will be made as to whether or not SWARM continues on to launch. The main function of the MAG is to formulate the detailed scientific requirements for the new mission and to draft a Mission Requirements Document.

SWARM is to provide the best description yet of the Earth's magnetic environment, including its particles, fields and currents, and how these change over time. These are important to our understanding of the interior of the Earth as well as the likely vulnerability of the Earth to periods of low magnetic field intensity. For example, it is now known that the Earth's main field is decaying at a rate faster than would be expected if the fluid motions in the core were suddenly switched off. This "forced decay" may be leading to a major reversal of the Earth's field.

SWARM will provide important new knowledge of the expanding, deepening South Atlantic Anomaly, with its serious implications for low-Earth satellite operations. Geographically, the recent decay of the Earth's magnetic dipole is largely due to changes in the field in that region. The geomagnetic field models resulting from this mission will have practical applications in many different areas, such as space weather and radiation hazards and understanding of atmospheric processes related to climate and weather.

The SWARM concept consists of a constellation of four satellites in two different polar orbits between 400 and 550 km altitude. Each satellite will provide high-precision and high-resolution measurements of the magnetic field. Together they will provide the necessary observations for the geomagnetic field that is needed to model its various sources.

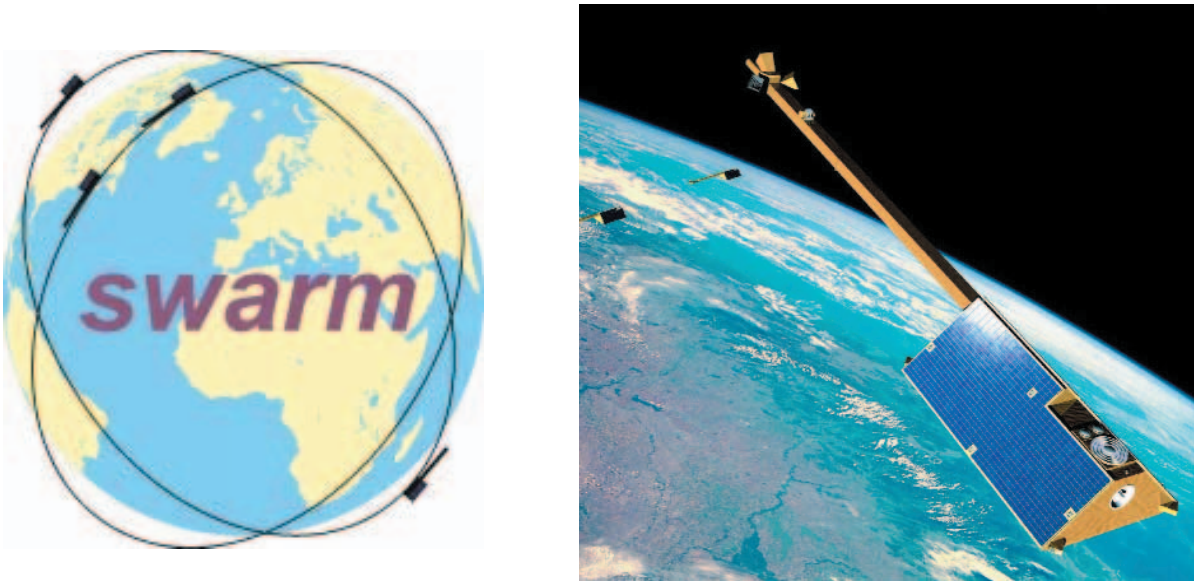

Figure 4. Left: SWARM logo. Right: Artist's concept of the SWARM constellation.

Contact: Mike Purucker, purucker@geomag.gsfc.nasa.gov

Four Attend Ørsted International Science Team Meeting

Figure 5.

In a strong show of the strength of the Goddard Geomagnetics Program, four members of the Lab for Terrestrial Physics (LTP) presented papers at the 4th Ørsted International Science Team meeting in Copenhagen, Denmark on 23-27 September 2002.

Pat Taylor (with co-authors Kim, Potts, von Frese and Frawley) gave a poster on "Satellite altitude geopotential study of the Kursk Magnetic Anomaly (KMA)" and was a co-author on a paper by Kim, von Frese, Park and Taylor "Utility of satellite magnetic observations for estimating near surface magnetic anomalies." Coerte Voorhies had a paper "Narrow scale, weak field flow at the top of Earth's core: evidence from Ørsted, Magsat and secular variation."

Mike Purucker presented along with Sabaka, Olsen and Maus his paper "How have Ørsted, CHAMP, and SAC-C improved our knowledge of the oceanic regions?" Terry Sabaka chaired a session and also gave a paper with Olsen on the "Comprehensive Modeling of the Earth's magnetic field: current status and future prospects". A paper on the most recent field model was published this year (see above).

In addition, Benoit Langlais, a post-doc from France working in the LTP, was a co-author on the paper by Hulot, Eymin, Langlais, Mandea and Olsen, "Small scale structure of the geodynamo inferred from Ørsted and Magsat satellite data", which was presented by Hulot.

Contact: Herb Frey, Herbert.V.Frey@nasa.gov

Magnetic Study of Rocks in the Kola and Krivoy Rog Deep Boreholes

In order to constrain the possible origin of satellite altitude crustal magnetic anomalies, information of the magnetic properties of rocks from the likely source regions is needed. Magnetic properties of rocks from two different boreholes, the Kola superdeep borehole and Krivoy Rog deep borehole, have recently been compared. Highly magnetic serpentinized peridotites and sedimentary rocks affected by sulfide mineralization were recovered at the Kola borehole at a depth interval of 1540-1940 m. The Krivoy Rog borehole recovered highly magnetic iron quartzites of Banded Iron Formations at depths of 1853-2040 m. Extremely high values of remanent magnetization (NRM), magnetic susceptibility (K) and Konigsberger ratio (Qn) are found at approximately the same depths of about 2000 m from both boreholes. There is no obvious reason why high magnetizations should occur at the same depth in two boreholes with such different lithologies. Magnetic surveys and surface sampling in the nearby Krivoy Rog and Kursk Magnetic Anomaly areas have revealed iron quartzites with high magnetization, similar to values given here. AF demagnetization tests suggest that a magnetically hard and stable NRM component, likely caused by hematite, occurred in iron quartzites in different forms and grain sizes ranges.

The data for this study can be found on the Goddard Magnetic Petrology Database now being compiled at the Geodynamics Branch of NASA/Goddard Space Flight Center and published on the web at: http://core2.gsfc.nasa.gov/research/terr_mag/php/MPDB/frames.html

A paper on this work has been submitted to Earth and Planetary Science Letters.

Contact: Katharine Nazarova, nazarova@geom.gsfc.nasa.gov

Narrow-Scale Flow at Top of Earth's Core

In previously published work [Voorhies, 1993, 1995], slow changes of the geomagnetic field were fitted in terms of broad-scale fluid flow by the top of Earth's liquid ferro-metallic outer core. These conditional core surface flow estimates indicate that the molten metal moves at about 8 km/yr. Analysis of magnetic changes from 1945 to 1980 revealed evidence for time-dependent flow by the top of the core, including a curious acceleration of fluid upwelling in an area 2900 km beneath Bermuda. If this acceleration were to continue past 1980, the intense upwelling would tend to blow away magnetic field line footpoints, weakening the magnetic field in this region. As it turned out, the greatest change in geomagnetic field intensity here on Earth's surface between the epoch 1980 Magsat mission and the epoch 2000 Ørsted mission was the 2400 nT (5%) drop in intensity centered on Bermuda.

Further work on the spectra of the main geomagnetic field and of its slow secular variation has revealed some evidence for narrow scale flow across a dynamically weak field. To test this hypothesis against observation, the Ørsted Initial Field Model is used to estimate the radius of Earth's core by spectral methods. The theoretical spectrum tested is obtained from the hypotheses of narrow scale flow across a dynamically weak magnetic field near the top of Earth's core. This describes a low degree, core-source magnetic energy range. Core radius c and amplitude K are estimated by fitting log-theoretical to log-observational spectra at low degrees. Estimates of c for degrees 4 through 12 are 3441 to 3542 km, which do not differ significantly from the seis-

mologic core radius (3480 km). Significant differences do occur if N exceeds 12, which is consistent with appreciable non-core source fields at degrees 13 and above (crustal fields). Similar results are obtained from the 1980 epoch Magsat model CM3. Also used was an expectation spectrum for low degree secular variation (SV) induced by narrow scale flow by the top of the core. The value of c obtained by fitting this form to the mean observational SV spectrum from model GSFC 9/80 is 3470 + 91 km, also in accord with seismologic estimates. This test of the narrow scale flow hypothesis is independent of the weak field hypothesis.

The results were summarized at the 2002 meeting of the Ørsted International Science Team and have been submitted to the Journal of Geophysical Research in the paper "Narrow scale, weak field flow by the top of Earth's core: Evidence from Magsat, Ørsted, and secular variation."

Contact: Coerte Voorhies, voorhies@geomag.gsfc.nasa.gov

Magsat, Ørsted and CHAMP Data Compared

Crustal magnetic anomaly signals are far weaker than either the Earth's main magnetic dipole field or the omnipresent time-varying external fields. In order to establish that these small amplitude, time-invariant magnetic signatures truly represented crustal units and therefore are useful in regional geologic and tectonic studies, it is useful to make satellite magnetic anomaly maps over well known magnetic features. Alternatively, upward-continued ground-based or aeromagnetic surveys can be compared with satellite data. When Magsat was launched in 1979, a satellite altitude (350 km) magnetic anomaly map over the well-known Kursk Magnetic Anomaly (KMA) region of Russia was produced by Taylor and Frawley (1987). The KMA (510 N, 370 E) has long been recognized as one of the largest magnetic anomalies on Earth. It is associated with massive quartz iron-ore formations (the largest known iron-ore deposits on Earth). In February 1999, the Ørsted satellite was launched (Neubert et al., 2001) into a much higher orbit (850 by 613 km) than Magsat. It was assumed by some that crustal magnetic anomalies would not be resolved. Taylor et al. (2000) showed, however, there was a distinct and similar crustal magnetic signal recoverable from Ørsted over this region (Figure 6). Following the launch of CHAMP into a circular 454 km orbit in July 2001, the initial data from this most recent mission was used to make yet another crustal anomaly map of the KMA (Figure 7).

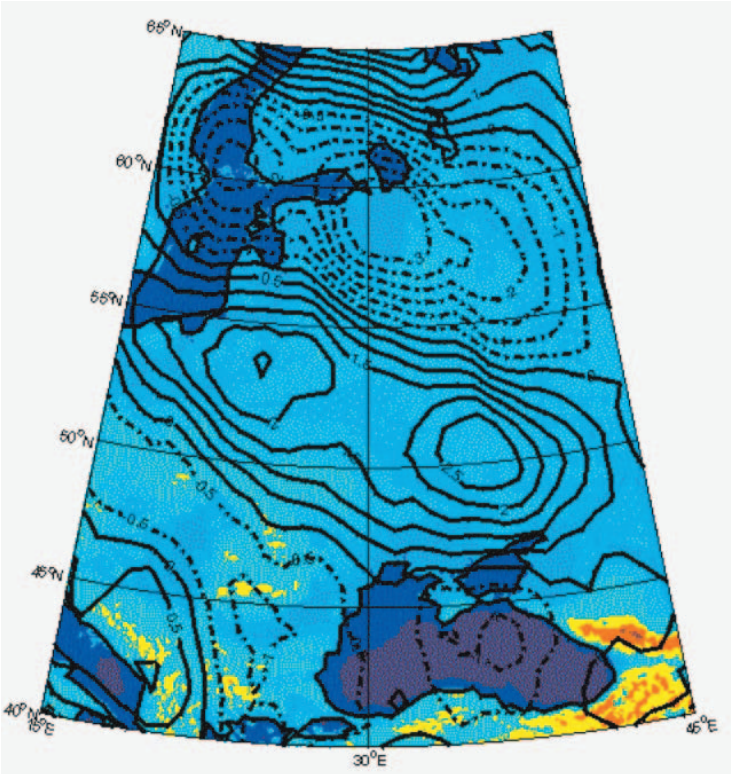

Figure 6. Anomaly maps of Magsat and CHAMP data plotted together over the KMA. Magsat contours are in a gray shade and the CHAMP contours are bolder. Contour interval is 3 nT with zero contour dotted and positive and negative values given by solid and dashed contours respectively.

Figure 7 shows the superposition of both the Magsat and CHAMP magnetic anomaly maps. Note that these anomaly contours over the KMA are very similar, having a generally northwest-southeast trend across this region and mirroring the iron-ore formations.

Differences between these anomaly fields are due to the greater number of orbit profiles from the CHAMP data set and different ranges of altitude and orbital eccentricities between these two satellites. Both the currently operating Ørsted and CHAMP geopotential satellites are able to record magnetic anomalies from sources within the Earth's crust and therefore can be used for geologic and tectonic studies. CHAMP is also recording the gravity field, so future studies will be able to incorporate the magnetic measurements with these gravity data to add another parameter to aid in our modeling of the crustal features of the Earth.

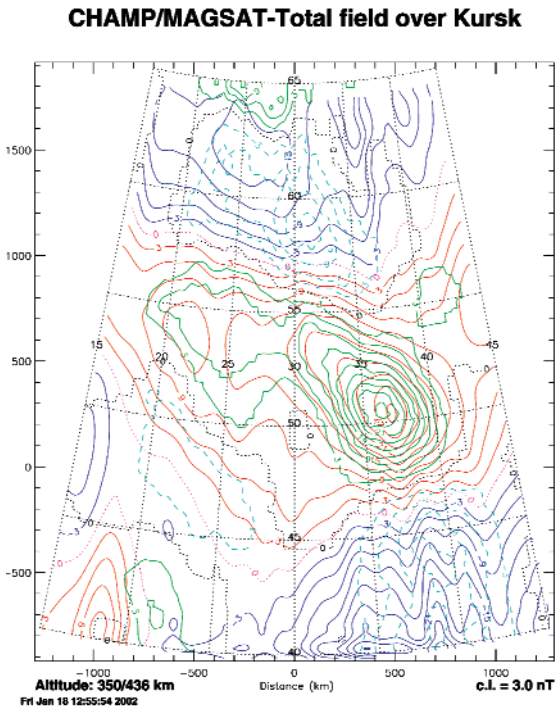

Figure 7. Anomaly maps of Magsat and CHAMP data plotted together over the KMA. Positive Magsat contours are green and positive CHAMP contours are red. Negative contours are blue, solid for CHAMP and dashed for Magsat. Contour interval is 3 nT with zero contour dotted.

[Report taken from: P. Taylor, H. Kim, R. von Frese, L. Potts and J. Frawley, Satellite-Altitude Geopotential Study of the Kursk Magnetic Anomaly (KMA), First CHAMP Mission Results for Gravity, Magnetic and Atmospheric Studies, edited by Ch. Reigber, H. Luehr and P. Schwintzer, Springer-Verlag, Heidelberg, in press, 2003]

References:

Neubert, T. et al. (2001): Ørsted Satellite Captures High-Precision Geomagnetic Field Data, Eos, Transactions, American Geophysical Union, 82, 81 and 87-88.

Taylor, P. T. and J. J. Frawley (1987): Magsat anomaly data over the Kursk region, USSR, Phys. Earth Planet. Interiors, 45, 5-15.

Taylor, P.T., R.R.B. von Frese and H. R. Kim (2000): Ørsted and Magsat: A comparison over the Kursk magnetic anomaly, Proceedings, 3rd Internantional Science Meeting, Grasse, France

Contact: Patrick Taylor, Geodynamics Branch, Patrick.Taylor@nasa.gov

Precise Orbit Determination, Gravity Field, and Terrestrial Reference Frame

Precision Orbit Determination Activities within The Space Geodesy Branch

Precise orbit determination (POD) is a major area of activity and expertise in the Lab for Terrestrial Physics (LTP). For some applications, as with satellite altimetry, POD enables science objectives such as the study of ocean, ice and land topography and surface change. In other applications, for example, reference frame and gravity field determination, science is derived directly from the precise determination of satellite orbits. Highlights below are some of the POD achievements of the LTP for the year 2002.

Jason-1 and TOPEX/Poseidon POD, Achieving the 1 cm Radial Orbit Accuracy Goal: Jason-1, launched on December 7, 2001, continues the time series of centimeter level ocean topography observations as the follow-on to the highly successful TOPEX/Poseidon (T/P) mission. The POD is critical to meeting the ocean topography goals of the mission. Fortunately, Jason-1 POD can rely on four independent tracking data types available including near continuous tracking data from the dual frequency codeless BlackJack Global Positioning System (GPS) receiver. Highly accurate orbit solutions have been computed using individual and various combinations of GPS, Satellite Laser Ranging (SLR) and Doppler Orbitography by Radio Positioning Integrated on Satellite (DORIS) data types from over 240 days of Jason-1 tracking data.

For nearly a decade NASA GSFC has computed the Precise Orbit Ephemerides (POEs) for the T/P mission based on SLR and DORIS tracking data. Building upon these capabilities, models and standards we have computed nearly 24 cycles (10-day repeat orbits) of Jason-1 POEs. Results from the recent Jason-1 Science Working Team meeting (Oct. 2002, New Orleans, LA) indicate these SLR/DORIS POEs are of the highest quality and show excellent agreement with high-fidelity POEs computed at other centers (e.g. JPL, CSR, CNES) and with other data types (e.g. our GPS computed orbits). Several improvements have been made in the SLR/DORIS POD including the calibration of the SLR tracking point offset with respect to the spacecraft center of mass and the development of an SLR/DORIS reduced dynamic solution strategy.

Also computed were highly precise orbits based on GPS data alone and in combination with SLR and DORIS tracking. Performance of the dynamic GPS based orbit solutions is excellent and suggests the 1 cm radial orbit accuracy mission goal is likely being achieved. Radial orbit overlap difference RMS is on the order of 7.3 mm (Figure 8) and independent high elevation SLR fit is 14 mm (Figure 9). The high elevation independent SLR residual performance is a good metric to gauge radial orbit accuracy, but the result does contain error sources other than radial orbit error. These orbit performance metrics alone indicate the GPS dynamic orbit solutions are highly precise and do not possess any significant systematic errors. Another valuable orbit performance test is to difference the SLR+DORIS orbit solutions with

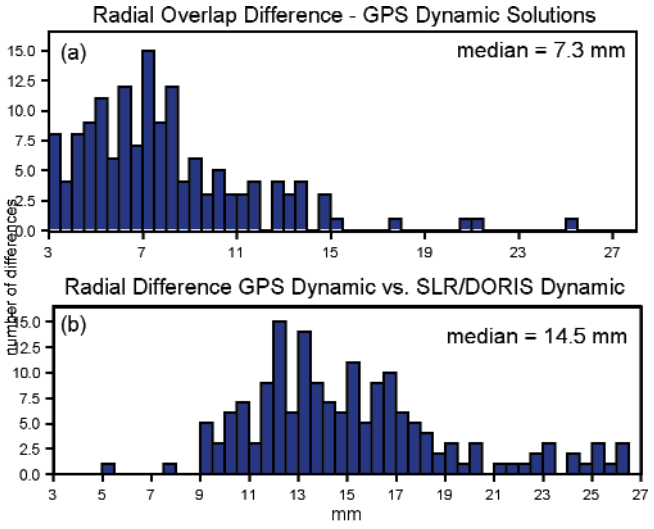

Figure 8. Jason-1 GPS dynamic solutions (30-hr. arc) (a) radial overlap difference and (b) radial difference with SLR/DORIS solutions.

the GPS based orbit solutions. This test can reveal tracking data and solution strategy dependent systematic orbit error. The orbits computed from the two sets of independent tracking data and orbit solution strategies show remarkable radial orbit agreement at the 14.5 mm level over the 190 days of orbit solutions compared (Figure 8). Ongoing analysis has shown further improvement in the GPS based orbit solutions has been obtained by employing a more aggressive reduced dynamic solution strategy (highly empirical parameterization).

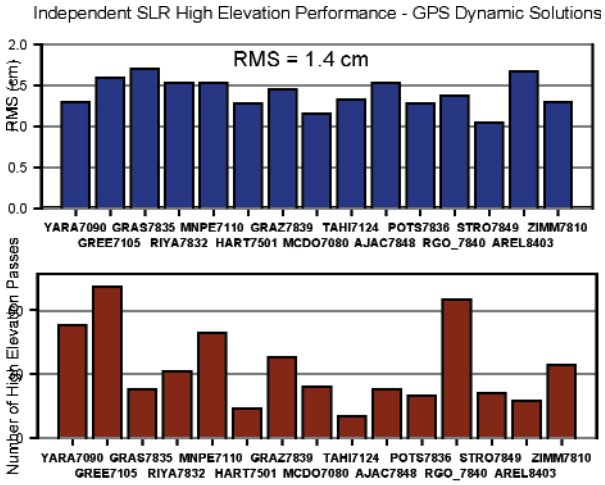

Figure 9. Jason-1 GPS dynamic orbit solutions (190, 30-hr. arcs) high elevation independent SLR performance

Although, Jason-1 will replace T/P it is important to continue to compute T/P precise orbit ephemerides as long as its altimeter remains active. Therefore, a tie between the Jason-1 and T/P missions can be established and a continuous history of ocean topography can be established. The LTP continues to compute the precise orbit ephemerides that are used on the geophysical data records (GDRs) of the T/P mission. T/P has been returning altimeter data almost continuously since October of 1992. Since then the Space LTP has computed more than 330 ten-day "cycles" of T/P orbits each with an accuracy of better than 3 cm radially and better than 15 cm in total position. The routine production of these highly accurate orbits has been a major factor in the success of the T/P mission.

POD for Earth Gravity Modeling (CHAMP and GRACE): The Laboratory has a very long history of extracting Earth gravity information from the analysis of satellite motion. With the launch of the German CHAMP (The Challenging Mini-satellite Payload) in 2000 and the launch of the US-German GRACE (The Gravity Recovery and Climate Experiment), the techniques by which gravity information is recovered from tracking data has dramatically changed and the LTP will help shape that change. These next generation gravity missions combine a new generation of GPS receivers, a high-precision three-axis accelerometer, and star cameras for the precision attitude determination. Accelerometer data is used to separate gravity perturbations from non-gravity perturbations after on-orbit calibration of the accelerometer. For the CHAMP mission, precision orbit determination based on GPS and SLR tracking data isolates the orbit perturbations, while GRACE includes inter-satellite ranging. We have processed over 90 days of CHAMP GPS, SLR and accelerometry data and has employed much of this data into new gravity solutions (see Gravity Model Development section). The state-of-the-art GPS and SLR tracking data analysis is complemented by the innovative accelerometer data analysis capabilities which are being applied to the on-orbit calibration of

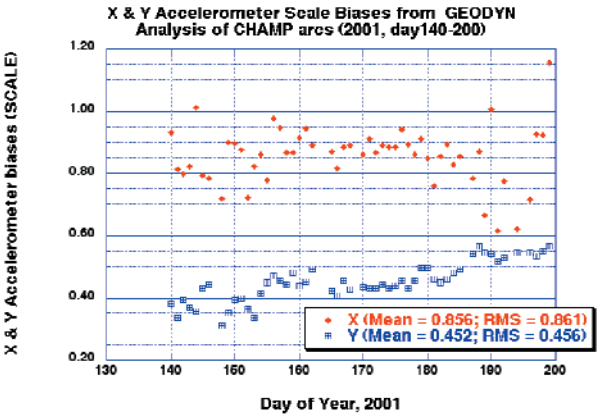

Figure 10. Calibration of CHAMP X and Y scale biases per each 30-hr. arc.

the CHAMP accelerometer. Figure 10 illustrates CHAMP accelerometer scale bias calibrations based on 30-hr. arc solutions. Figure 11 shows the CHAMP post-fit GPS double difference ionosphere-free carrier phase residuals for each 30-hr. arc processed (5025811 observations; median RMS = 0.83 cm). Figure 12 presents histograms of CHAMP radial overlap RMS (median = 0.82 cm) and independent SLR fit RMS (median = 4.1 cm) for each 30-hr. arc solution.

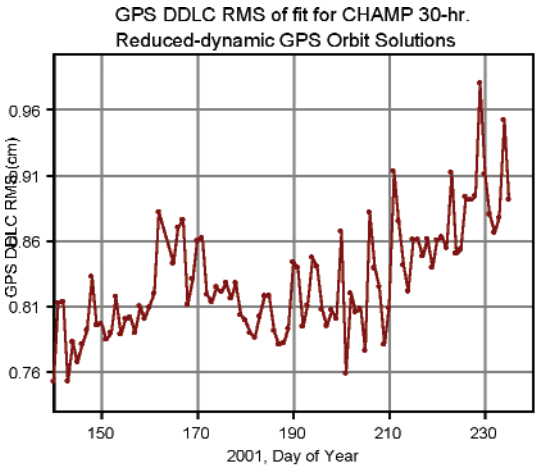

Figure 11. Champ GPS DDLC post-fit RMS per 30-hr. arc.

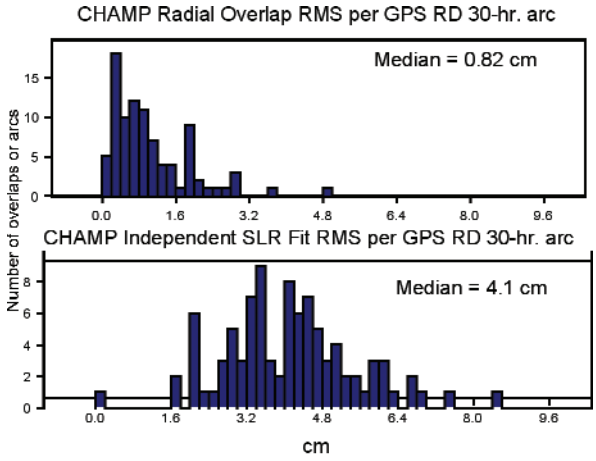

Figure 12. Radial overlap performance (top) and independent SLR fit RMS per 30-hr. arc (bottom)

POD for Laser Altimetry (SLA, MGS, ICESat): Orbit determination for laser altimeter satellites brings with it a unique set of challenges and possibilities. Laser altimeters require on-orbit calibration of instrument parameters such as pointing and ranging biases. The Laboratory has developed an approach that simultaneously determines the orbit of a satellite along with the laser altimeter instrument parameters from a combined reduction of navigation tracking and laser altimeter range data. These capabilities have been applied to Mars Global Surveyor orbit determination and altimetric calibration and was an integral part of Mars topographic mapping and geopotential development. In preparation for future earth observing space-based laser altimeter missions, this approach has been successfully applied to the reduction of Shuttle Laser Altimeter (SLA-01 and SLA-02) mission tracking and altimeter ranging data significantly improving the orbits and geolocation. In 2002, the focus was on refining these capabilities and developing and assessing POD and geolocation calibration and validation strategies in preparation for the January 12, 2003 ICESat launch.

GEOSAT Follow On (GFO): GFO is a radar altimeter satellite. The satellite belongs to the Navy, but the data is available to the scientific community. By an agreement with the Department of the Navy and the National Oceanic and Atmospheric Administration (NOAA), the Laboratory is funded to compute the precise orbit ephemeredes for GFO. The GPS receivers on GFO have not been performing at a usable level and we are one of the very few groups capable of achieving near TOPEX/Poseidon level accuracy for GFO without GPS tracking. This is in part due to the dynamic crossover capability. GFO-GFO dynamic crossovers are routinely used in our GFO orbit solutions and were also used to "tune" a gravity field for GFO. In 2002, the Laboratory continued to routinely produce the GFO precision orbits that have enabled scientific research across government agencies.

Contact: David Rowlands, David.D.Rowlands@nasa.gov

Detection of a Large Scale Mass Redistribution in the Terrestrial System since 1998, and an Assessment of the Potential Causes.

The recent results of Cox and Chao [2002] identified a significant departure from the otherwise linear post-glacial rebound (PGR) dominated drift in the Earth's J_2 zonal harmonic. That analysis included Satellite Laser Ranging (SLR) data from a total of 10 different satellites, covering the period from 1979 up to 2002, and has since been extended through 2002. The recovered series includes J2 through J4, as well as some sectorial and tesseral signals describing longitudinal gravity variations.

Figure 13 shows the complete data series. With the exception of the additional data in 2002, it is similar to Figure 2 of Cox and Chao [2002]. In addition to the J_2 zonal, the time series for J_3 was also estimated. The J_3 zonal, which describes north-south mass distribution, does not show any significant anomalies corresponding to the timing of the J_2 event. There are indications that J_2 is returning to the nominal values and long-term trend dictated by post-glacial rebound. Consequently, the deviation may be interannual in nature, and therefore does not necessarily represent a departure from the long-term trend.

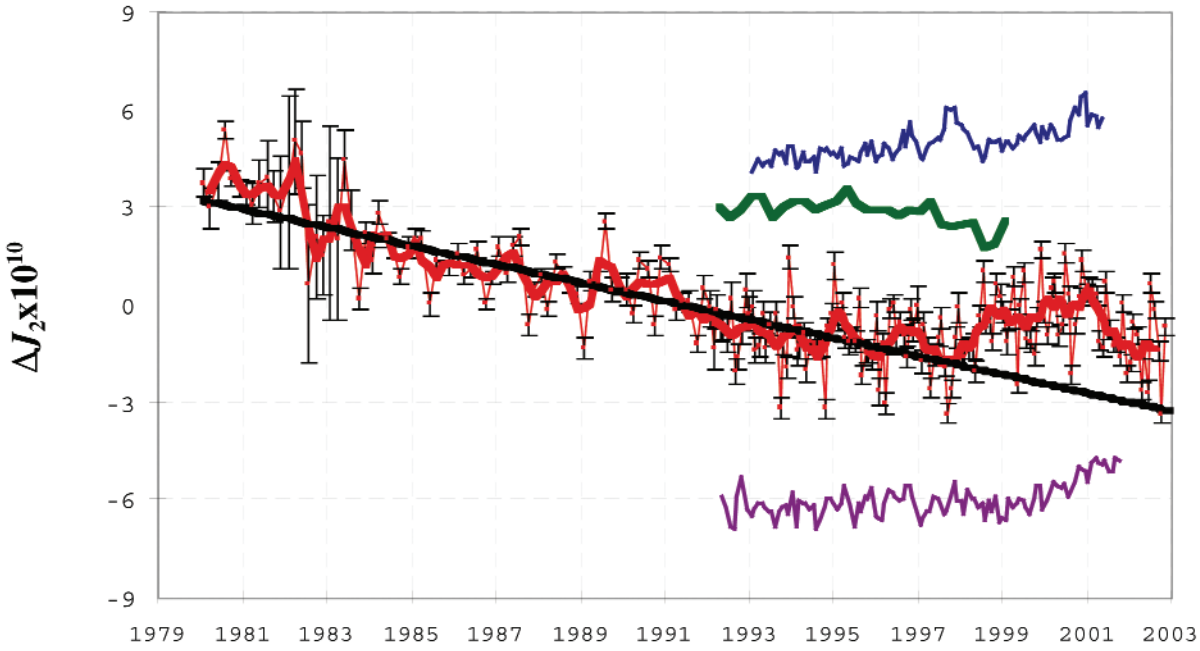

Figure 13. Observed ΔJ_2, after subtraction of the IB corrected atmospheric signal and an empirical annual term, before (thin red line with error bars) and after an annual filter has been applied (heavy red line). Error bars are the observed J_2, uncertainties. The heavy black line is a weighted fit to the (unfiltered) pre-1997 data. The slope is -2.8×10^{-11} year^{-1}. The offset green line (second from top) is the J_2 implied by the Greenland + W. Antarctic ice heights derived from ERS-1/2 altimetry data. Also shown are the J_2 implied by the T/P uniform Global Sea Level change (blue, offset, top), and that considering the geographic distribution of the sea height changes (purple, offset, bottom). Neither sea height derived estimate includes steric effects. Sampling intervals are 90-days in 1979, 60-days from 1980 through 1991, and 30-day afterwards. No detrending of rates has been performed. Units are 10^{-10}.

The atmospheric gravity correction applied to the data in Figure 13 was computed from the monthly National Center for Environmental Predictions (NCEP) reanalysis pressure grids assuming a two-dimensional approximation. While the atmosphere explains a good portion of the variation from the monthly to annual periods, it does not explain the anomaly. The maximum difference between the two-dimensional and three-dimensional computations amounts to ~0.5×10^{-10}

change in the annual amplitude, with no significant effect on the interannual variation.

Ice melting scenarios large enough to explain this deviation produce a large Global Sea Level change (~2 mm/yr above the pre 1998 rate), which simply has not been observed. Likewise, the apparent recent turn in J_2 would then imply a recent accumulation of ice mass, which, while not impossible, is unlikely. Terrestrial water impoundment is another possible factor. Large dams can individually cause a jump of ~0.2×10^{-10} in J_2, however, the cumulative effect since 1998 is far too small to explain the observed J_2 changes. Regrettably there is insufficient reliable data at the moment to make any assessment about the role of hydrology. Review of geodynamo model output showed that under some assumptions rates as large as ~$0.5\text{-}1.0 \times 10^{-11}$ per year are possible. While the core signal may be larger than previously assumed, it still does not explain the J_2 anomaly.

There is evidence that some component of the cause of the J_2 anomaly lies within the oceans. The timing corresponds to changes in the primary empirical orthogonal function (EOF) modes for the sea surface temperature (SST) and sea surface height (SSH) in the extra-tropic regions (See Figure 14a and 14b). The primary SST EOF mode corresponds to the Pacific Decadal Oscillation (PDO), which is generally correlated with the J_2 series. The timing also corresponds to changes in the primary EOF modes of the ECCO ocean model [Stammer et al., 1999] bottom pressure (Figure 14c and14d). Analysis of the ECCO assimilation run output shows that the most influential region is the Southern Pacific, although some effects are also seen in the other regions. However, the ECCO ocean model bottom pressure data can only explain about 25% of the observed magnitude of the J_2 change. Nonetheless, the good overall agreement in the timing and nature of the event with the ocean activity warrants more detailed analysis of the ocean's role.

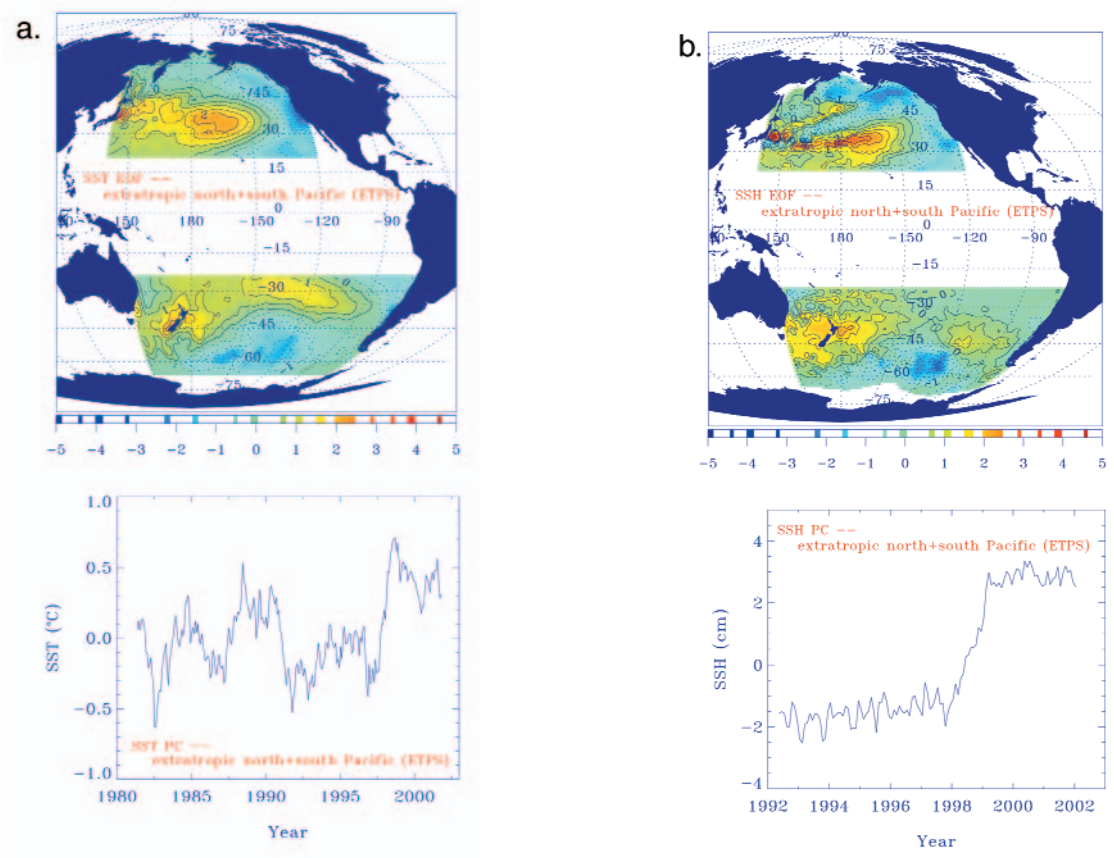

Figure 14. Primary modes of EOF/PC analyses of the (a) Reynold's Sea Surface Temperature, (b) T/P Sea Surface Height for the extratropic regions of the Pacific Ocean.

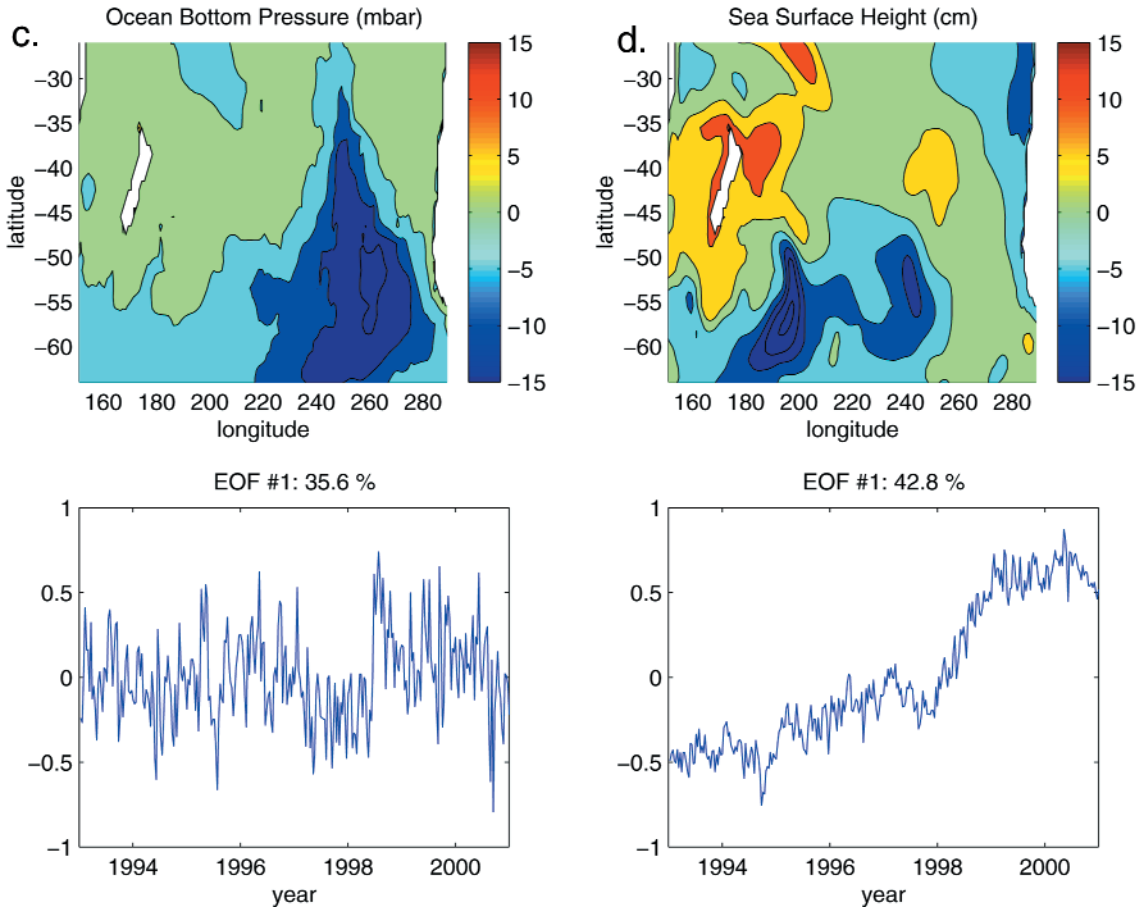

Figure 14. (c) ECCO ocean bottom pressure, and (d) ECCO sea surface height from the assimilation model for the South Pacific. For each panel, the top figure shows the spatial component of the mode, while the bottom panel shows the time series of the scalar component.

Contact: Christopher Cox, ccox@stokes.gsfc.nasa.gov

Earth Geopotential Solutions from CHAMP Satellite Data

The CHAMP (CHAllenging Minisatellite Payload) spacecraft, launched in July 2000, is the first in a series of missions that will revolutionize the ability to model the Earth's geopotential. The CHAMP mission, managed by the GeoForschungsZentrum (GFZ), Potsdam, Germany, orbits the Earth at altitudes of 400 – 450 km at a near polar inclination. The spacecraft is equipped for precision tracking with the global positioning system (GPS), and satellite laser ranging (SLR). In addition, CHAMP carries a precision accelerometer to measure the nonconservative forces acting on the spacecraft. More than ninety days of CHAMP GPS, SLR, and accelerometry data (from days 140 to 230 of 2001) has been processed using our GEODYN orbit determination software. These data have been used to estimate solutions for the Earth's geopotential that are a substantial improvement over earlier solutions based on pre-CHAMP data (for example, EGM96, JGM-2, JGM-3).

The processing of the CHAMP data involves several steps. First, is to determine the best possible orbits using a reduced-dynamic technique for a series of 30-hr arcs. Second, is the calibration of the accelerometer to determine the appropriate scale and absolute biases. Velocity impulses are estimated to account for the numerous attitude maneuvers experienced by the CHAMP spacecraft, which have no expression in the smoothed accelerometer data provided by GFZ. Normal

equations are created to 120 x 120 in spherical harmonics on the Cray SV1 and the HP/Compaq SC45 supercomputers at NASA GSFC's National Center for the Computational Sciences. So far, we estimated test solutions to 90x90 using between 10 and 40 days of data.

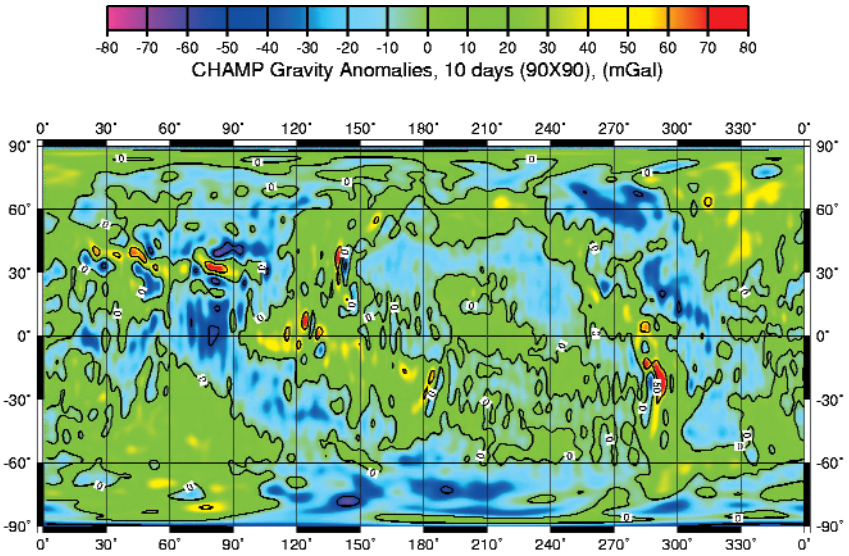

Figure 15: Gravity Anomalies to 90x90 from ten days of CHAMP data.

Figure 15 illustrates the anomalies from a 90 x 90 solution based on CHAMP data from May 20-30, 2001. This solution was based on only 368,814 GPS double difference observations. While the solution will not have as much detail as a high degree solution that includes altimetry or surface gravity (such as EGM96), a fair amount of detail is discernible from only ten-days of CHAMP data.

Figure 16 illustrates the degree variances from two satellite-only geopotential solutions: EGM96S, based solely on pre-CHAMP tracking data (such as SLR, GPS, DORIS, TDRSS, Tranet Doppler), and PGS7760B, a test solution based on only forty days of CHAMP data. The EGM96S solution is deficient in power above degree 40-45 due to the lack of homogeneous and high-quality global coverage. In contrast, the CHAMP test solution does not lose power at the high degrees. In fact, the upturn in the power spectrum is a signature of aliasing and an indication the CHAMP solutions should be extended beyond degree 90.

An independent altimeter-derived anomaly was used to test the satellite-only geopotential solutions by comparing the discrepancies at degree 70 between the anomalies predicted by these geopotential solutions, and the gravity anomalies derived from ocean radar altimeter data. It was found that for the pre-CHAMP solution, EGM96S, the discrepancy has a variance of 10.19 $mGal^2$, whereas for the CHAMP satellite-only test solution the anomaly discrepancy has a variance of 4.57 $mGal^2$. This single test implies that even a few months of CHAMP data have greater strength than the space geodetic tracking data collected over the previous thirty years of the space age. This conclusion has an important caveat, namely that a CHAMP-only solution will not represent faithfully the resonance to which different satellites may be sensitive, so that the best solution will still require CHAMP data to be merged with other tracking data, e.g. from JASON, ICESAT, STARLETTE and other satellites.

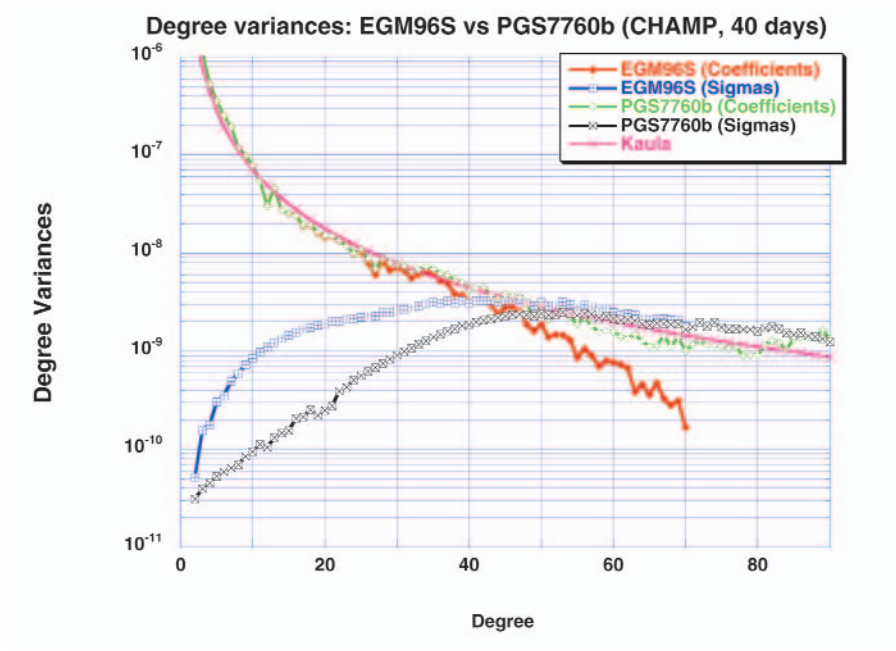

Figure 16: Degree variances for satellite-only geopotential solutions.

Contact: Frank Lemoine, Frank.G.Lemoine@nasa.gov

The NASA Geodetic/Astrometric VLBI Program

The capabilities of Very Long Baseline Interferometry (VLBI) have been developed and continually improved over the past 35 years, and NASA continues to be a major sponsor of the geodetic and spacecraft applications through programs at Goddard Space Flight Center and at the Jet Propulsion Laboratory. It is appropriate that as NASA expands its program in Earth system studies, NASA also continues to take the lead in advancing the space geodetic techniques, which will contribute so significantly to Earth sciences in the coming decades.

VLBI has three important attributes: unique determination of the Celestial Reference Frame (CRF) and the orientation of the Earth in that frame, accuracy, and long-term stability. Only through these VLBI measurements can many of the properties of the Earth's interior be inferred, such as: dynamical oblateness of the core-mantle boundary, magnetic properties of the inner and outer cores, and anelasticity of the mantle. The CRF provides the precise background for deep space navigation of spacecraft and alignment of catalogs at different observing frequencies.

The VLBI definition of the scale of the Terrestrial Reference Frame (TRF), measurement of UT1-UTC, and the long term stability of the reference system and orientation of Earth in space are fundamental requirements for the geodetic measurements by all other techniques. Led by the NASA team, the technological developments that have brought VLBI to its present level of accuracy are the result of international collaboration and support.

Continual technology improvement is the basis of all experimental advances and will provide both better accuracy and more rapid delivery of results. For the global geodetic VLBI program the technology advances have been due to the leadership of the VLBI groups at GSFC and at the MIT Haystack Observatory operating under a NASA contract. The implementation of these projects has been the product of large international collaborations involving many countries and agencies. Current technology emphasis is aimed at two initiatives. The first is the Mark 5 disk-based data

acquisition system, which will benefit the science through better sensitivity while reducing costs and improving reliability. The second is the use of high bandwidth optical fiber communication for real-time VLBI, first demonstrated by the Communications Research Laboratory of Japan.

Mark 4 correlators have been operational at the United States Naval Observatory (USNO), the Max Planck Institute for Radioastronomy (MPIR), the Joint Institute for VLBI in Europe (JIVE), and Haystack for about three years and have now completely replaced all Mark III and Mark IIIA correlators. Over the last year, significant enhancements have been made to Mark 4 correlator software to improve operational flexibility and efficiency. The Mark 4 correlator is now designated as 'mature', but further enhancements are still possible.

The Mark 5 disc-based data system is well along in development and entered field operation in 2002; approximately 20 Mark 5P units have been deployed. In addition, the Mark 5 system was used in a demonstration of ~1 Gbps electronic transmission of VLBI data over an IP network between Haystack Observatory (Westford, MA) and NASA/GSFC, a distance of ~700 km.

Based on the success of the Mark 5 demonstration unit shown in 2001, NASA (under contract with Haystack Observatory) is now undertaking the development of an operational 1 Gbps Mark 5 system with support from other cooperating partners: Bundesamt fuer Kartographie und Geodaesie (BKG, Federal Agency for Cartography and Geodesy, Germany), Korean VLBI Network (KVN), MPIR, JIVE, National Radio Astronomy Observatory (NRAO) and USNO.

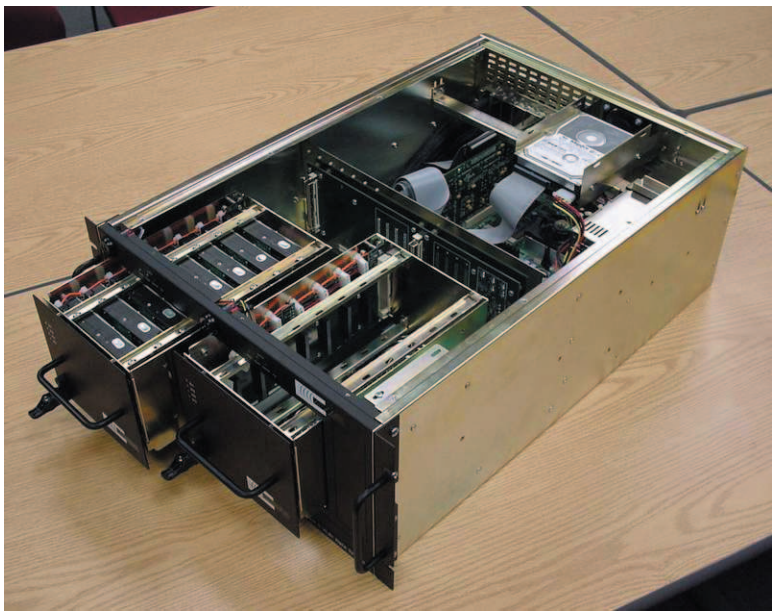

Figure 17. Mark 5 disk-based VLBI data recorder.

e-VLBI Development

NASA and DARPA supported Haystack Observatory to demonstrate 1-Gbps e-VLBI over a standard IP-based network between Haystack Observatory and NASA/GSFC. Part of the network path was over standard U.S. science network infrastructure, where other users share the network links and the data must traverse many routers and switches. One purpose of this test was to determine the real throughput of these networks under stressful shared conditions. Tests between Haystack Observatory and the Westford antenna already demonstrated sustained data rates of ~980 Mbps over standard Gigabit Ethernet links through several switches. The Westford antenna at Haystack Observatory was used in conjunction with the GGAO antenna at NASA/GSFC.

In two tests in October VLBI data were transmitted from both antennas to the Mark 4 correlator at Haystack Observatory for correlation. In the first test the data were first recorded on Mark 5P and then transmitted at ~788 Mbps to Haystack for rebuffering and correlation. In a second test the GGAO data were transmitted real-time to Haystack.

The first intercontinental e-VLBI fringes were achieved between Kashima, Japan and Westford in October buffered on a K5 disk-based recorder in Japan and a Mark 5P at Westford. Data were transmitted in both directions and correlated at both ends with normal results. Although the data rates were only ~1.5 Mbps, the rates should improve substantially in the future. The intention is to seek support to extend Gbps e-VLBI to other sites within the U.S. as well as overseas to Europe. Paths between Hawaii and Washington, DC and between the U.S. and Germany are being organized for further tests.

Contact: Chopo Ma, Chopo.Ma@nasa.gov

International VLBI Service (IVS)

The GSFC Very Long Baseline Interferometry (VLBI) group has been actively involved in initiating and participating in the International VLBI Service for Geodesy and Astrometry (IVS). This aligns with NASA's efforts for the development of partnerships within industry, government and the international community in sharing resources.

The IVS is a service of the International Association of Geodesy (IAG), International Astronomical Union (IAU) and Federation of Astronomical and Geophysical Data Analysis Services (FAGS). The charter and the basis for international collaboration is given by the Terms of Reference (ToR) accepted by IAG and IAU and by the proposals provided by individual agencies in response to the call of participation. IVS is an international collaboration of organizations that operate or support VLBI components.

The IVS inauguration date was March 1, 1999. IVS is tasked by IAG and IAU for the provision of timely, highly accurate products Earth Orientation Parameters (EOPs), Terrestrial Reference Frame (TRF), Celestial Reference Frame (CRF), etc. IVS has no funds of its own and is dependent on the support of individual agencies that responded to the call for participation.

The IVS Coordinating Center is based at GFSC and is operated by NEOS (National Earth Orientation Service), a joint effort for VLBI by the U.S. Naval Observatory and NASA GSFC. The mission of the Coordinating Center is to provide communications and information for the IVS community and the greater scientific community and to coordinate the day-to-day and long-term activities of IVS. GSFC provides the web server for the Coordinating Center. The address is http://ivscc.gsfc.nasa.gov

During 2002, the VLBI group processed and analyzed 164 24-hr geodetic/astrometric sessions and 192 1-hr UT1 Intensive sessions. The 24-hr sessions included the weekly R1 and R4 observations for monitoring of EOP. In addition 15 continuous CONT02 sessions were scheduled in October using Gilmore Creek, Alaska; Kokee Park, Hawaii; Algonquin, Ontario; Westford, Massachusetts; Ny Alesund, Norway; Wettzell, Germany; Hartebeesthoek, South Africa, and Onsala, Sweden. Analysis was begun as the sessions became available from the correlators, and the quality of the data is quite good. These sessions will provide information for high frequency and transient phenomena in Earth orientation and station motions.

Analysis staff collaborated with NRAO and Caltech personnel to perform the astrometric analysis of two new VLBA calibrator survey experiments and determined milli-arcsecond level positions of 276 additional calibrator sources, many of which can be used in geodetic VLBI sessions. A paper with the first 1332 source positions was published. Analysis staff collaborated with USNO, JPL, and NRAO personnel to process and analyze VLBI survey observations at K band

(23 GHz) and Q band (44 GHz). These observations are the beginning of the work to generate a Ka band (34 GHz) catalog to support future spacecraft navigation and to extend the microwave celestial reference frame to other frequencies.

VLBI solutions were used to study ocean loading. Position variations of 40 VLBI stations at 32 tidal frequencies were obtained from analysis of 3 million measurements of group delays from 1980 to 2002. It was found that the estimates of station displacements are generally in a good agreement with the ocean loading computed on the basis of ocean tide models for the main diurnal and semi-diurnal tides. However, discrepancies between VLBI results and all models of ocean loading for K1, K2 and S2 tides exceed both the errors of the VLBI estimates and the errors of ocean loading displacements based on the reported formal uncertainties of ocean tide models. It was found that there is a significant non-tidal signal at diurnal and annual frequencies. Applying a model of hydrological loading reduces the variance of the residual vertical displacements at the annual frequency by 30%.

The large VLBI analysis package Calc/Solve was maintained, upgraded, and distributed to the IVS community bimonthly. The capability to access the NCEP reanalysis weather model and to calculate atmosphere loading was added to the VLBI analysis system. The transfer of the code of Solve from a HP Unix platform to a Linux platform was begun to make the system available to more users.

Contact: Chopo Ma, Chopo.Ma@nasa.gov

Crustal Dynamics Data Information System (CDDIS)

The CDDIS is a dedicated data center supporting the international scientific community as NASA's space geodesy data archive since 1982. This data archive was initially conceived to support NASA's Crustal Dynamics Project. Since the end of this successful program in 1991, the CDDIS has continued to support the science community through NASA's Solid Earth and Natural Hazards program, HQ Code YS. The CDDIS provides easy and ready access to a variety of data sets, products, and information about these data. The CDDIS archive includes Global Positioning System (GPS), GLObal NAvigation Satellite System (GLONASS), Satellite Laser Ranging (SLR), Very Long Baseline Interferometry (VLBI), and Doppler Orbitography and Radiolocation Integrated by Satellite (DORIS) data and products. The specialized nature of the CDDIS lends itself well to enhancement to accommodate diverse data sets and user requirements. Information about the system is available at http://cddisa.gsfc.nasa.gov.

The CDDIS serves as one of the primary data centers for the following services within the International Association of Geodesy (IAG):

International GPS Service (IGS) and its diverse pilot projects and working groups

International Laser Ranging Service (ILRS)

International VLBI Service for Geodesy and Astrometry (IVS)

International Earth Rotation Service (IERS)

International DORIS Service (IDS)

The CDDIS is operational on a dedicated computer facility located in Building 33 at NASA GSFC. This computer facility hosts web sites for the CDDIS, the ILRS, and several other GSFC facilities. The majority of the CDDIS data holdings are accessible through anonymous ftp and the web.

By the end of 2002, users had downloaded over 40 million files, averaging over 250 Gbytes in size each month. Furthermore, nearly 200 users accessed the CDDIS on a daily basis to download data. Nearly ninety countries accessed and downloaded data from the CDDIS last year. Over 120 institutions in over sixty countries supply data to the CDDIS on a daily basis for archival and distribution to the international user community.

CDDIS Activities in 2002

In support of the IGS pilot project on Low Earth Orbiter (LEO) missions, the CDDIS enhanced its archive to include GPS data from flight receivers on-board SAC-C and CHAMP. Data from ICESat and JASON will be archived in 2003. Analysts will retrieve these data to produce precise orbits of these LEO platforms, which will aid in the generation of other products, such as temperature and water vapor profiles in the neutral atmosphere and ionosphere imaging products. The IGS LEO Pilot Project will test the ability of the various components of the IGS infrastructure to support near real-time acquisition, dissemination, and processing of GPS data.

The CDDIS began archiving data from continuously-operated GPS receivers located at or near tide gauge instruments in support of another IGS pilot project, TIGA-PP, or the Tide Gauge Benchmark Monitoring Pilot Project. Analysts using these data will produce time series of coordinates for studying vertical motions of tide gauges and tide gauge benchmarks.

The CDDIS staff assisted in the publication of several ILRS documents, particularly the 2000 and 2001 annual reports and the updated ILRS brochure.

New Thrusts for the CDDIS

Providing funds are available, a new LINUX-based system will be purchased to replace the current UNIX server. This system will be equipped with one or two RAID disk arrays (nearing one TB of on-line disk space) and optionally a dedicated tape backup system.

Website: http://cddisa.gsfc.nasa.gov/cddis_welcome.html

Contact: Carey E. Noll, Carey.E.Noll@nasa.gov

Improved Mapping Functions for Atmospheric Corrections in Satellite Laser Ranging

An accuracy-limiting factor in modern space geodetic techniques, such as the Global Positioning System (GPS), Very Long Baseline Interferometry (VLBI), and Satellite Laser Ranging (SLR), is atmospheric refraction. The atmospheric refraction modeling at radio wavelengths has improved significantly in the last decade, in contrast to that for optical wavelengths, where the standard for data analysis is still the 1970s Marini-Murray refraction model. A better atmospheric refraction model is of great importance in reducing the error budget in SLR measurements in high-precision geodetic and geophysical applications. For example, the study of spatial and temporal variations in the Earth's gravity field, the monitoring of vertical crustal motion, and the prospect of a more robust combination of solutions from different space techniques.

Two new mapping functions (MFs) were developed to better model the elevation angle and observational wavelength dependence of the atmospheric delay for SLR data analysis. The new MFs were derived from ray tracing through a set of data from 180 radiosonde stations globally distributed, for the year 1999, and are valid for elevation angles above 3°. When compared against ray tracing of two independent years of radiosonde data (1997-1998) for the same set of stations, the

MFs reveal sub-millimeter accuracy for elevation angles above 10º, representing a significant improvement over other MFs. This is confirmed in improved data reductions of LAGEOS and LAGEOS 2 SLR data from the Int. Laser Ranging Service (ILRS) global tracking network.

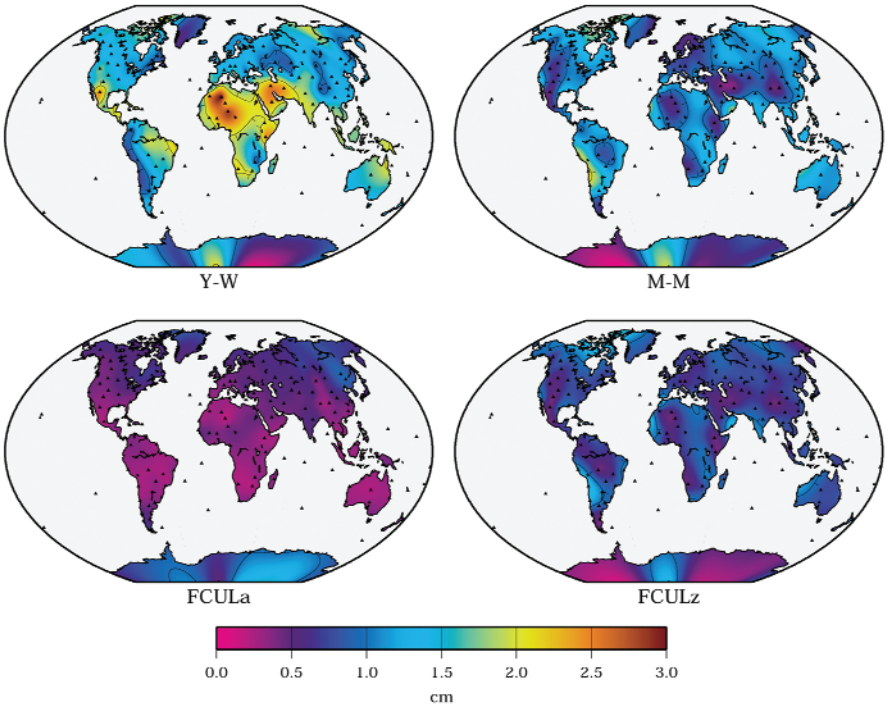

Figure 18. Two-year average r.m.s. differences: model predictions minus ray tracing, at 10 degrees elevation angle. Plots on the left represent MF errors for our new MF "FCUL2000a" and the MF of Yan and Wang; plots on the right represent the combined error of zenith delay modeling (ZD) and MF errors for the Marini-Murray and our model FCUL2000z.

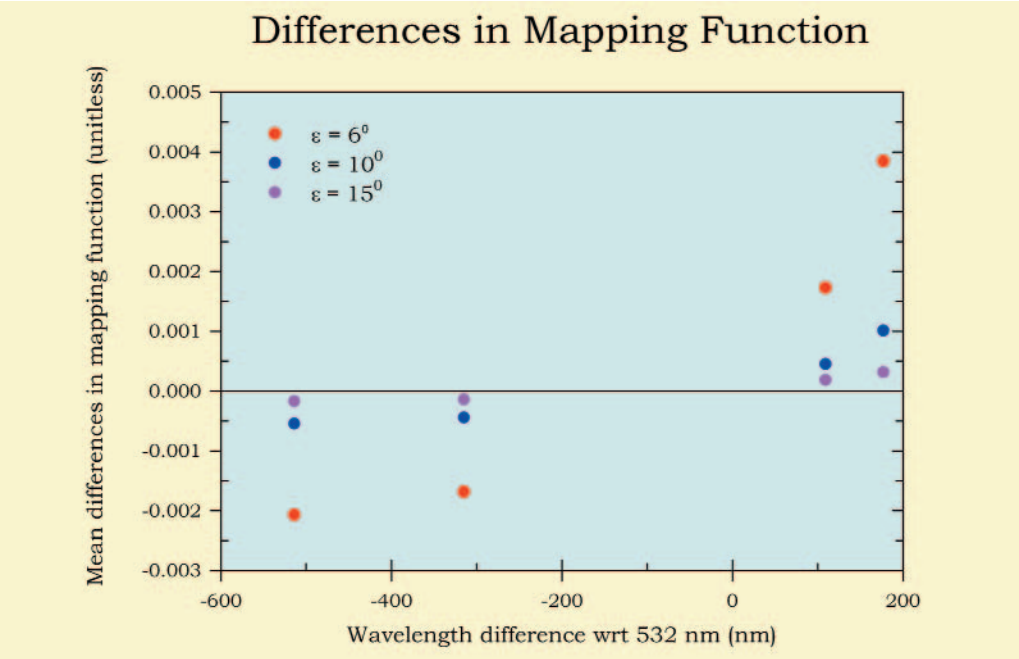

Figure 19. Mean differences in the mapping function scale factor with respect to nominal wavelength of 532 nm. The worst departure is at 355 nm and for a nominal 2.5 m correction, corresponds to 1 cm.

Table 1. RMS for Mapping Functions (e = 10°), in the sense "model minus ray tracing" (cm).

λ	Full models		Mapping functions ONLY		
(nm)	Marini-Murray	FCULz	FCULa	Yan-Wang	Saastamoinen
355	1.77	3.83	0.55	1.72	3.04
423	0.79	0.75	0.46	1.65	2.48
532	1.14	0.82	0.41	1.56	2.16
847	1.05	0.75	0.39	1.56	2.05
1064	0.98	0.62	0.39	1.77	2.06

Reference:

Mendes, V.B., G. Prates, E.C. Pavlis, D. E. Pavlis, and R.B. Langley "Improved mapping functions for atmospheric refraction correction in SLR" Geophysical Research Lett., 29(10), 1414, doi:10.1029/2001GL014394, 2002.

Contact: Erricos Pavlis, epavlis@JCET.umbc.edu

Absolute Earth Scale from SLR Measurements

Since the LAGEOS I satellite was launched in 1976, the systematic instrument error of the best satellite laser ranging observatories has been steadily reduced. Advances in overall system accuracy, in conjunction with improved satellite, Earth, orbit perturbation and relativity modeling, now allows us to determine the value of the geocentric gravitational coefficient (GM) to less than a part per billion (ppb). This precision has been confirmed by observations of the LAGEOS II satellite, and is supported by results from Starlette, albeit at a lower level of precision. When observations are considered from other geodetic satellites orbiting at a variety of altitudes and carrying more complex retro-reflector arrays, consistent measures are obtained of scale, based upon empirically determined, satellite-dependent detector characteristics. The adoption of a value of GM differing by a ppb would result in a difference of a few millimeters in the height definition of a near-Earth satellite. The precision of the estimate of GM from satellite laser ranging has improved by an order of magnitude in each of the last two decades.

The Evolution of Scale Definition

During the 1970s, the determination of the Earth's geocentric gravitational coefficient was independently determined from observations of several interplanetary spacecraft, including the Ranger, Surveyor, Lunar Orbiter, Pioneer, Mariner and Viking flights. The analysis of the first six months of LAGEOS I data was shown on a vertical scale with a full range of 1 km^3/sec^2, corresponding to the sixth decimal digit of GM, and equivalent to about one part per million. The early, decimeter-accuracy LAGEOS observations were included in the development of the GEM-L2 gravity model, most of whose data was collected in the 1970's, when the prevailing scale knowledge was based on the speed of light 299729.5 km/sec. An uncertainty of 0.02 km^3/sec^2 (50 parts per billion) was assigned to the new estimate for GM with a value of 398600.44 km^3/sec^2 after appropriate scaling for the speed of light currently adopted (299729.458 km./sec).

Improvement in Scale Definition

LAGEOS I and II data collected between 1986 and 1992 were used to determine the IERS92 standard. The data collected since 1990 suggested higher estimates of GM with generally better con-

sistency from each LAGEOS satellite. The average value for LAGEOS II was 498600.44187 km^3/sec^2, which was chosen as the most appropriate value from this analysis. The scatter of annual determinations of GM from several other geodetic satellites over a four-year period was found to contribute no absolute scale information, but their scatter provided an indication of overall network consistency for the tracking of these satellites.

Latest Results

In a recent analysis, ten years of data from LAGEOS I and II were combined to simultaneously estimate independent values of GM at monthly interval. The scatter (standard deviations) about the mean of the monthly values shown in Figure 20 gives a realistic error measure of about one-half part per billion, and the formal errors of single estimates give optimistic assessments. The formal errors would hold if the ranging observations were randomly distributed about the orbits at the level of the final residual fit for each satellite. The orbit fits are about 3 cm for LAGEOS I and II and the orbital residuals are not random. The high range residual level is caused by unmodeled Earth, satellite and orbit errors. As these models improve in the future, the associated uncertainty in the scale parameters will be reduced. The inclusion of a more precise pressure measurements yielded a GM value which is about one half ppb higher than the adopted standard which is just within the quoted uncertainty.

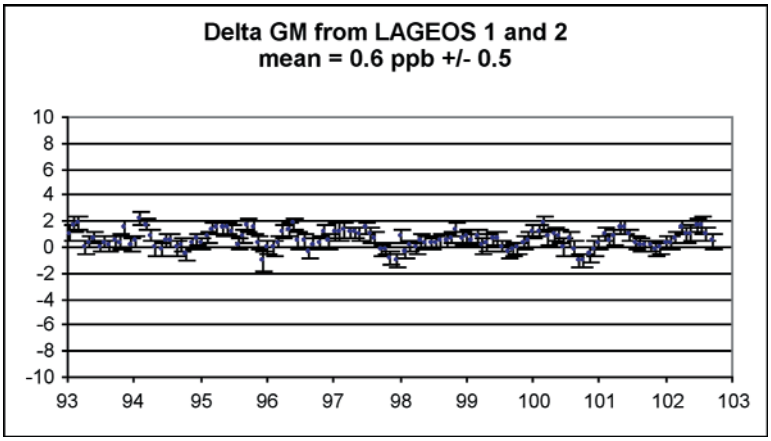

Figure 20. Determination of Scale from a Recent Analysis

Scientific Relevance of Earth Scale Determination:

Satellite geodesy depends on the integrity of the geocentric gravitational coefficient for its definition of scale. An accurate value of the universal gravitational constant times the mass of the Earth (GM) enables us to monitor the behavior of the Earth, as sensed by satellite observations, in an absolute reference frame. Improved orbit scale definition provides an important component to the definition of the geopotential model, and has among its most practical applications a contribution to the refinement of the positioning of altimeter satellites, which carry stringent radial accuracy requirements. This work will help to define the long-term stability of the SLR reference frame and improve the positioning capability of the network. The rate of sea level rise caused by global warming is currently measured over decade time scales with tide gauges, which provide observations relative to the Earth's surface. The scale inherent in laser ranging observations to stable high-altitude satellites enables us to determine accurate geocentric height at the observatories. The work also contributes to the refinement of the positioning of altimeter satellites, which carry stringent radial accuracy requirements in order to define sea level relative to the Earth's center. Furthermore, we anticipate that routine monitoring of Earth processes to which ranging scale is sensitive, such as seasonal and secular variability in Earth albedo, can also provide important indicators of the effects of global change.

Contact: Ronald Kolenkiewicz, Ronald.Kolenkiewicz-1@nasa.gov

Kinematic GPS Activity within the Laboratory for Terrestrial Physics

Kinematic positioning is a technique that takes advantage of the simultaneous visibility of four or more GPS satellites, from anywhere and at any time, to find the position of moving vehicles without knowing their actual dynamics. It is an extremely versatile technique, as exemplified by the topics of recent studies carried out in cooperation with colleagues at other organizations. These include: The Polytechnic University of Catalonia (UPC) (on improving GPS-based navigation with atmospheric models); the Navy's Naval Surface Warfare Center (NSWC) at Dahlgren, the UPC, the University of Alicante, and the University of Tasmania (on the precise location of buoys at sea for satellite altimeter calibration), and the University of Nagoya, and the Japan Hydrographic Department (on sea-floor tectonics).

Low Earth Orbiter (LEO) Trajectory Determination:

Another project is to find a way to use kinematic GPS for precise positioning of LEOs equipped with GPS receivers. Some new ideas are being tested. The most recent is, first to use long-range kinematic GPS (lacking dynamic constraints), and then make an orbit fit (constrained by orbit dynamics) to the resulting trajectory, in order to filter out the kinematic errors. These errors tend to be rather large in satellite trajectories, because both the fast-changing subset of GPS spacecraft in view from the LEO, and the very long baselines between this and the fixed ground stations, together make ambiguity floating imprecise, and ambiguity fixing unreliable. The procedure outlined here requires a relatively small number of ground sites distributed around the world, selected from the much larger set of IGS stations on the basis of their consistently good performance. This method could be useful when processing altimetry and other satellite data requiring good orbit registration. The technique has been implemented almost entirely with software already available at the Branch. It has been tested making two 24-hour orbit estimates for the oceanographic satellite TOPEX/Poseidon, and another two, for the satellite JASON. The estimated orbits agree to better than 5 cm RMS in height and 17 cm in three-dimensional RMS with the NASA Goddard Space Flight Center Precise Orbit Estimates (POE), which are also produced at the Branch (see section on POE). The results are summed up in the Table below (from a paper Colombo, Luthcke, Rowlands, Poulose, and Chin, in the Proceedings of ION GPS 2002). Those POE have been derived exclusively from DORIS Doppler and laser tracking data, so they provide an entirely independent way to verify GPS-based results.

Work continues on improving the purely kinematic solutions. The goal is to use dynamics-free kinematic solutions to check the dynamically determined POEs for systematic errors, to detect problems and, perhaps, help validate the force models used.

Table 2. Departure of Dynamic Orbit Fit from GSFC's POE (Centimeters)

TOPEX

DAY	RSS	dR (RMS)	dR MEAN	Points in Orbit Fit
12/14/93	14.6	3.8	0.2	1801
06/24/95	8.6	1.4	0.2	1766

JASON

DAY	RSS	dR RMS	dR MEAN	SLR RMS	Points in Orbit Fit
08/04/02	15.1	4.5	-0.3	9.9	1242
09/04/02	15.1	4.8	0.1	9.5	1367

Contact: Oscar Colombo, ocolombo@olympus.gsfc.nasa.gov

Global Geophysical Fluids

Application of Core Dynamics Modeling to Geodetic Studies

Earth's outer core is the largest geophysical fluid system (in both volume and mass). Its temporal and spatial variations interact with other geophysical processes and generate global geodynamic changes that can be measured via space geodetic technologies. A well-known example is the length of day (LOD) variation of the Earth. Geomagnetic observations demonstrated that LOD variation on decadal time scales results from exchange of axial angular momentum between the Earth's core and the solid mantle. This core-mantle angular momentum exchange is a product of core-mantle interactions. Therefore, multi-disciplinary studies in geodynamo, geodesy and geomagnetism could help not only interpreting geodetic/geomagnetic observations, but also furthering the understandings of core dynamics.

During 2002, efforts were continued in the application of the MoSST core dynamics "geodynamo" model on dynamics of core-mantle interactions. In addition to complete the research in electromagnetic core-mantle coupling (two papers are in preparation), research was begun in gravitational core-mantle coupling that arises from mantle and outer core density anomalies with two actions. The first is the development of a module to calculate gravity field anomalies of the mantle, and the resultant gravitational torque. The second is a construction of a mantle density anomaly model from seismic observations (reported at EGU/AGU Joint Assembly in Nice, France). In collaborating with recent progress on time-varying gravity measurements (e.g. J_2 series), gravity variation was also analyzed due to core fluid density anomalies with the MoSST model. With various parameters and exclusion of possible effect of mantle deformation due to pressure variation at the Core-Mantle Boundary (CMB) (internal loading), it was found that core fluid density anomalies (due to convection) could contribute to a very complicated time-varying gravity field at the Earth's surface (see Figure 21). In particular, the J_2 component could be as large as 10^{-10}/year, and could partially explain the observational results. Findings suggest that time-varying gravity measurements could also be used in core dynamics studies by providing possible constraints on density variation (and thus buoyancy force) in the fluid outer core, thus opening a new method of detecting dynamics of the Earth's deep interior.

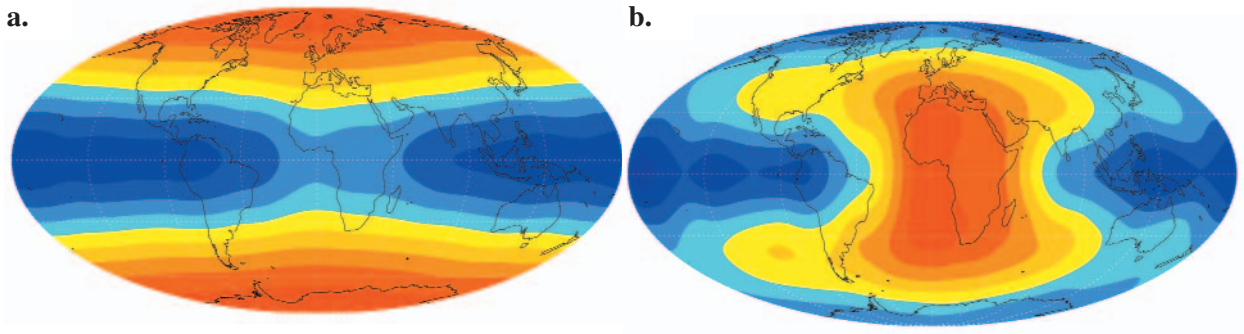

Figure 21. Snapshots of time-varying gravity anomaly (i.e. the departure of the gravity field from the Earth's mean gravity field) at the Earth's surface due to core fluid density variations: (a) the total gravity anomaly that demonstrates a dominant J_2 component, (b) the non J_2 part of gravity anomaly, showing significant spatial variation due to higher order gravity anomalies. The orange and blue colors represent the anomaly above and below the mean field, respectively.

Contact: Weijia Kuang, Weijia.Kuang-1@nasa.gov

Precise Atmospheric Loading Estimates for New Space Gravity Missions.

The new space gravity missions will provide gravity field measurements with unprecedented precision and high spatial resolution. The retrieval of oceanic and hydrological signals from the monthly time-variable gravity field recovered by the GRACE satellites requires a precise knowledge of the atmospheric contributions.

The atmosphere being nearly hydrostatic at low frequencies, the atmospheric thickness is usually neglected and the atmospheric loading is therefore modeled using only the surface pressure and a thin-layer (2-D) assumption. Because of the new requirements in accuracy, this traditional approach is no longer sufficient for deducing atmospheric loading effects and have to model the effects induced by the three-dimensional (3-D) structure of the atmosphere.

The 3-D structure of the air density has been reconstructed from the classical meteorological parameters (pressure, temperature and specific humidity) on a realistic topography provided by meteorological centers such as NCEP (National Center for Environmental Predictions). Using these global meteorological datasets has shown that the differences between the 2-D and 3-D approaches are larger than the expected GRACE sensitivity (Figure 22) up to harmonic degrees of 20-40 (corresponding to wavelengths of 1000-2000 kilometers) and hence should be taken into account.

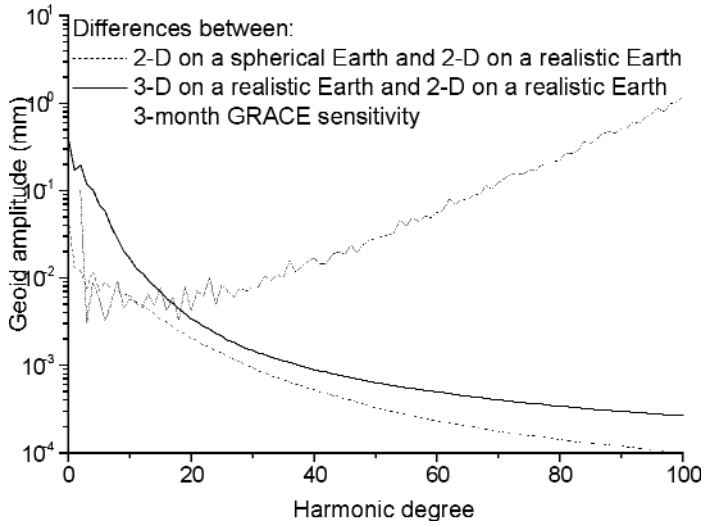

Figure 22. Spectrum of the geoid height RMS differences between the 2-D approximations and 3-D loading, according to NCEP Operational and for April 2002 through June 2002.

Also shown is the 3-D atmospheric loading that is not only required for estimating the high frequency atmospheric contributions on Earth's gravity field variations but also for longer periods for the zonal harmonic coefficients, mainly at annual and semi-annual timescales.

Contact: Jean-Paul Boy, boy@bowie.gsfc.nasa.gov

Crustal Deformation

Earth Anelasticity from Satellite Tracking and Altimetry

The moon and sun raise tides not only in the oceans, but also in the solid Earth. These "Earth tides" have long attracted the interest of geophysicists, partly because they hold the promise of revealing unknown properties of the Earth's deep interior. For example, one long-sought goal has been to determine the anelastic properties of the deep interior. Those properties are known fairly well at seismic frequencies, but not at lower frequencies, so studies of Earth tides, especially those of diurnal and semidiurnal periods, could help close this gap in understanding the Earth's response to large-scale forces. Unfortunately, all previous Earth-tide studies have failed to determine the tidal anelastic effect because the signal is very small and hidden by the much larger ocean-tide signals.

A recent analysis of space geodesy data has now determined the anelastic lag in the Earth tide. This was done by combining satellite tracking data, primarily laser tracking of LAGEOS and other geodetic satellites, with satellite altimeter data, primarily from TOPEX/POSEIDON. The tracking data are senstive to the gravitational effect of tides, while the altimeter data are sensitive to the direct geometric effect. By themselves neither data type can separate the ocean tide from the Earth tide, but combining the two data types allows a clean separation.

Analysis of the principal semidiurnal tide (period 12.4 hours) reveals an Earth tide lag of 0.102°±0.023°, corresponding to a time lag of about 25 seconds between maximum tidal forcing and maximum Earth-tide elevation. This implies a solid-earth Q of about 300.

Similar determinations for other tides will hopefully allow us to determine the variation of Q as a function of frequency, a key property of the Earth's deep interior.

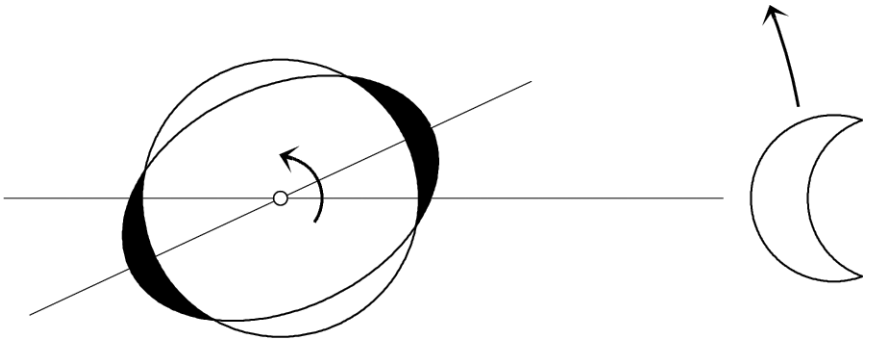

Figure 23. Because of anelasticity the Earth's tidal bulge lags the moon's tidal force, while the Earth's rotation sweeps this lagged bulge ahead of the moon. The lag in the Earth tide has been determined to be about 0.1°. For comparion, the lag in the ocean tide is almost 65° and has hitherto hidden the small Earth-tide.

Reference:

Ray, R. D., R. J. Eanes, and F. G. Lemoine, "Constraints on energy dissipation in the Earth's body tide from satellite tracking and altimetry," Geophysical Journal International, vol. 144, pp. 471-480, 2001.

Contact: Richard Ray, Richard.D.Ray@nasa.gov

Invited Review Summary of South Central Alaska Crustal Deformation

The 1964 Alaska earthquake is the largest known seismic event (moment magnitude, Mw=9.2) to strike North America and the second largest event to occur anywhere in the world within the modern observational era. The region of south central Alaska that was directly affected by this earthquake (i.e. from Cordova to Kodiak Island and Anchorage to well offshore, see Figure 24) lies at the boundary between the converging Pacific and North America tectonic plates. Over the past few decades a tremendous body of scientific information has been developed about the earthquake cycle in this region that has given new insight into how strain is accumulated and released in subduction zones. The temporal and spatial pattern of crustal deformation that has been revealed is far more complex than predicted by extant models of plate boundary zone seismicity. The editors of the series "Advances in Geophysics", have asked Steve Cohen to prepare for publication a comprehensive summary of crustal deformation in southcentral Alaska. The summary is based not only on the decade long observational and modeling study he has carried out, but also on studies from other investigators.

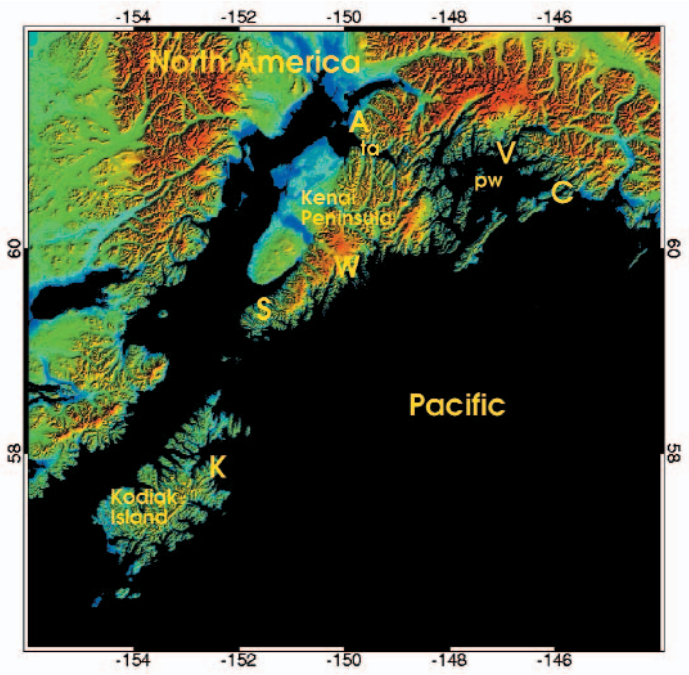

Figure 24. Topographic rendition of Southcentral Alaska. Cities shown by letters are A=Anchorage, C=Cordova, K=Kodiac, S=Seldovia, V=Valdez, W=Seward. Also ta=Turnagain Arm and pw=Prince William Sound.

The available geodetic data is a rich mixture of space age and conventional observations. For the past decade Global Positioning System (GPS) studies of point positions have provided data used to derive estimates of horizontal and vertical crustal velocities. Areas of special concentration have included the Kenai Peninsula, nearby offshore locations, the greater Anchorage area, the Kodiak Island-Katmai region to the southwest, and near Valdez to the east. Prior to the availability of GPS, precision level surveys were undertaken to provide information on vertical motion. Repeated surveys were conducted along the Turnagain Arm, and single epoch measurements are available on the Kenai Peninsula. Tide gauge measurements have been made more or less continuously at a half dozen or more coastal sites. In a few cases, these measurements provide a time series extending back to before the 1964 earthquake. Very Long Baseline Interferometry (VLBI) measurements were made in the late 1980's on Kodiak Island and at a few other sites in Alaska. Recently, a continuously operating GPS station was installed near the tide gauge at Seldovia.

Additional information about crustal movements come from a limited number of triangulation measurements, tsunami records, and geological observations such as changes in the heights of algae and soil depositional changes.

Some of the most significant results from this wealth of data include:

(1) The postseismic uplift in the region that subsided during the earthquake was both rapid and large. Between Anchorage and the Kenai Peninsula the subsidence was as much 2m during the earthquake. However, the cumulative uplift since the earthquake may exceed 1m in some locales (Figure 25). The most rapid uplift was right after the earthquake and may have been as much as 150 mm/yr. Leveling data from the Turnagain Arm suggests that postseismic creep occurred along the down-dip extension of the coseismic rupture plane in the first few years following the earthquake. On the other hand, decreases in the vertical displacement rate at tide gauges on Kodiak Island and Cordova reveal the existence of a much longer-lived transient phenomenon lasting on the order of 1-2 decades. Other tide gauge data suggest that an even longer lived post-seismic process may also be at work.

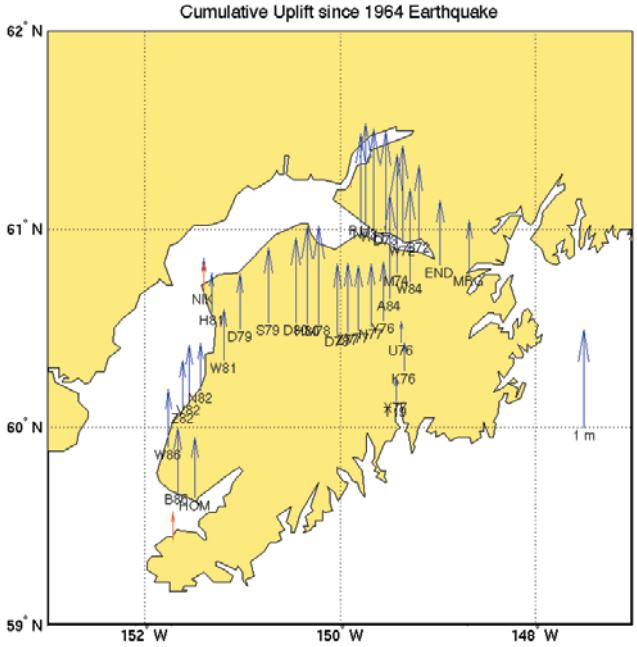

Figure 25. Uplift since 1964 on Kenai Peninsula and adjacent areas. The uplift is plotted relative to a tide gauge station at Seward. The red arrows show uplift as determined from tide gauge observations, the blue arrows show uplift determined by comparing post-earthquake leveling height observations to contemporary GPS vertical position determinations.

(2) There is considerable along-strike (lateral) variability in the contemporary pattern of horizontal deformation. On the eastern Kenai Peninsula, the present-day velocities (relative to stable North America) are as large as 30-40 mm/yr. These are parallel to the direction of relative plate motion, decrease with distance from the plate boundary, and are largely consistent with standard models of strain accumulation along a strongly coupled plate interface. However, in the western Kenai Peninsula, the velocities are directed SSW, i.e. generally in the opposite direction from those on the eastern side of the Peninsula, and have speeds on the order of 20 mm/yr. The pattern of crustal deformation is suggestive of a long-lived or delayed response to the 1964 earthquake, but does not allow for significant contemporary strain accumulation.

(3) There can be sudden changes in the deformation pattern even several decades after the earth-

quake. GPS measurements near Anchorage made prior to 1998 display a velocity pattern similar to those on the Kenai Peninsula and are indicative of strain accumulation. However, the velocities reversed after 1998 and it appears that a "slow earthquake," with considerable slip, may well have occurred.

Taken as a whole, these observations suggest a complex pattern of plate boundary interactions where the coupling between the overriding and subduction plates not only varies with location but also with time. Thus the models of regional seismotectonics that are required today are much more sophisticated than the simple elastic-frictional or even viscoelastic-frictional models of just a few years ago. Researchers are now developing various numerical models of this crustal deformation that take into account both bulk rock properties and fault rheology, variations in the plate interface geometry, and both plate interface and crustal faulting. The "Advances in Geophysics" article is a comprehensive summary of both the observational information and modeling results from the southcentral Alaska region that will serve as a resource for investigators studying both the Alaskan as well as other subduction zones.

Contact: Steve Cohen, Steven.C.Cohen@nasa.gov

Topography and Surface Change

Puget Sound Lidar Studies

Surface deformation caused by large earthquakes often produces geomorphic features that provide significant constraints on fault locations, sense of motion, and displacement magnitudes. David Harding, a participant in the Puget Sound Lidar Consortium (http://www.pugetsoundlidar.org), is using very high resolution digital elevation data in the Puget Lowland of Washington State to characterize deformation caused by Holocene earthquakes. The elevation data was acquired by airborne laser mapping, a technique that reveals the ground topography beneath the dense temperate rain forest cover of the Pacific Northwest.

At invited talks this year at the Geological Society of America Cordilleran Section annual meeting, the Spring American Geophysical Union meeting, and the Geological Society of Washington, Harding reported on results that define spatial patterns of fault slip that occurred circa A.D. 900 in the Seattle fault zone. This slip was due to a magnitude 7 (or greater, earthquake). Harding used the laser mapping data to measure the elevation of shoreline angles at the landward edge of uplifted and tilted terraces that border Puget Sound (Figure 26). A shoreline angle is a paleo-horizontal marker originally formed at sea level by wave-cut erosion. The terraces define a broad, 5 km wide, asymmetric anticline across the width of the Seattle fault zone, formed by slip on the most northerly, basal thrust.

The terrace offsets on the south limb of the anticline indicate that structural higher thrusts also underwent slip during the earthquake. This study documents that multiple fault strands within the Seattle fault zone are still active and constrains their magnitude and sense of slip during the A.D. 900 earthquake. These results contribute to an improved assessment of the earthquake hazard in the densely populated Puget Sound region.

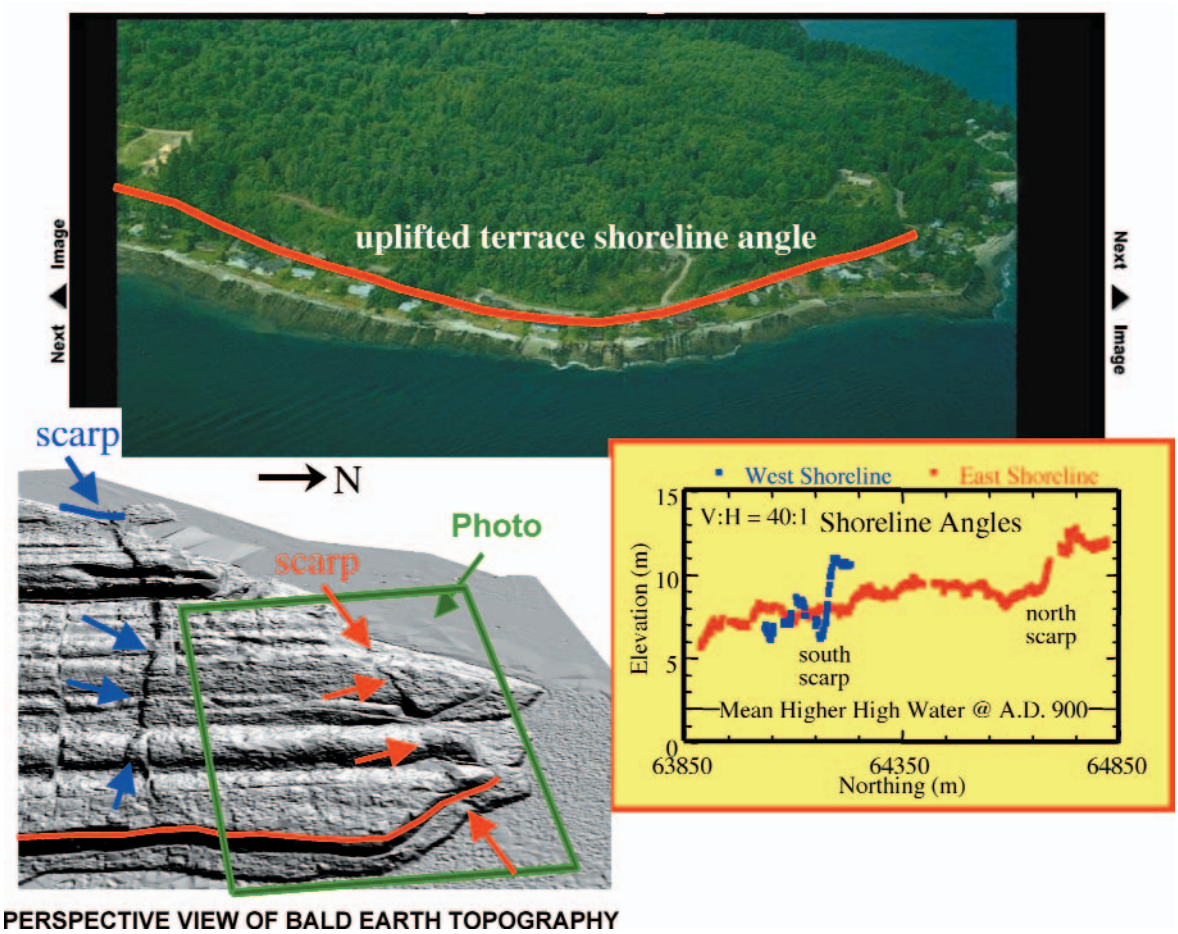

Figure 26. An example of terrace shoreline angle elevation profiles (lower right) measured from laser mapping elevation data (lower left) that reveals the ground topography beneath dense vegetation (the north-south ridges are the result of glacial erosion). The terrace was uplifted by as much as 10 m, tilted to the south, and offset by fault scarps during the A.D. 900 earthquake.

Contact: David Harding, David.J.Harding@nasa.gov

Quantifying Plains Volcanism on the Eastern Snake River Plains and Mars

Basaltic plains style volcanism is a common form of volcanic planetary resurfacing, and is thought to be a significant factor in the volcanic and thermal histories of all of the terrestrial planets (Earth, Moon, Mercury, Mars, and Venus, as well as some of the larger satellites of the Gas giants). Plains volcanism is well illustrated on Earth, with perhaps the textbook example being the Eastern Snake River Plains (ESRP) of Idaho. Volcanic features in the ESRP have erupted through several hundred separate vents, and are characterized by a mix of rift eruptions, low shields that often coalesce, a few cinder cones, and extensive fields of relatively thin lava flows. Commonly the flows were slowly emplaced through systems of channels and lava tubes over rather low regional slopes. The total thickness of the sequence is thought to be a few km, erupted over about 15 million years, with the most recent eruptions within the last few thousand years, and future eruptions possible at wide time intervals.

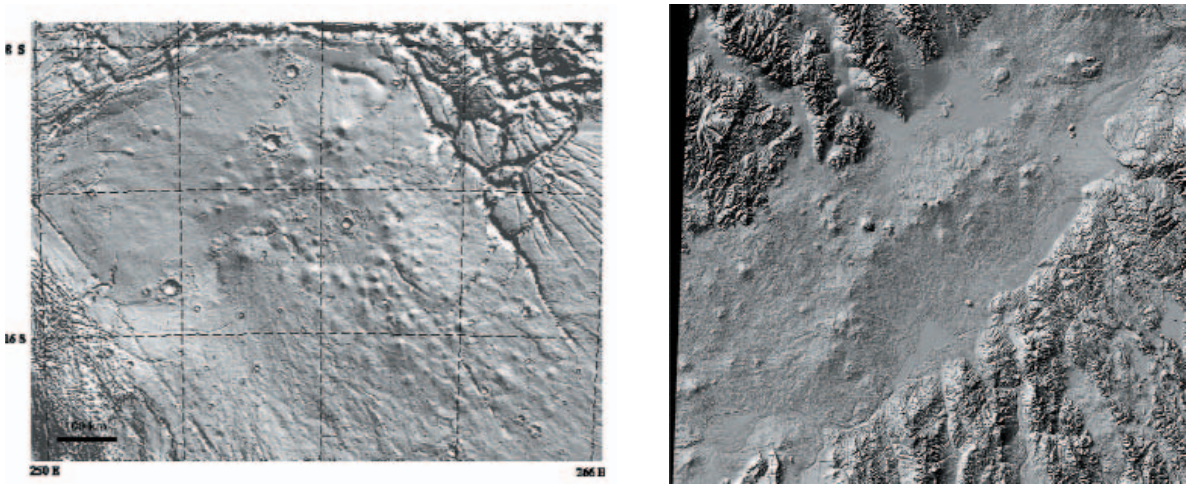

Figure 28. Shaded relief topography for the Syria region of Mars (left) and the Eastern Snake River Plains region of Idaho (right). Both regions show basaltic plains volcanism features, including low shields, flow fields, lava tubes, and rift eruptions.

While this style of volcanism is well known, it is not yet well understood or quantified even though it is important for the understanding of regional terrestrial resurfacing rates, volcanic hazards, and tectonic-volcanic systems relationships. Susan Sakimoto and colleagues Tracy Gregg (SUNY, Buffalo) and Scott Hughes (Idaho State) are engaged in the study, which combines existing remote sensing measurements with higher accuracy field measurements and ground truth to understand the topography and petrology or the ESRP system, and to use that data to constrain eruption types and rates. In parallel with the terrestrial measurement effort, they are characterizing similar regions on Mars, with the expectation that terrestrial results will be directly applicable to the similar martian rate and eruption style questions. The work is in collaboration with the Idaho Space Grant, and is funded through both the NASA Space Grant EPSCoR 2000 program and through the NASA Mars Data Analysis Program.

This past summer, the field season in the ESRP was focused on using GPS receivers to characterize topography profiles across the summit regions of the low volcanic shields as well as across some of the tube and channel fed volcanic flows. The summit regions show some systematic differences in topography that appear to be correlated with the petrology (texture and composition) of the lavas. This may be a direct reflection of the chemical evolution of the contributing magma chamber (e.g. Hughes, et al., 1999, 2001, 2002a, 2002b). The field data combined with remote spectral and topographic data and laboratory compositional and petrological work suggests that the steeper summit regions on many of the basaltic shields are very likely an expression of the slightly more evolved petrology for these shields, and in some cases are diagnostic of the extent of local ground water involvement in the eruption process. The parallel work on the topography of the martian volcanic fields (e.g. Sakimoto et al., 2001, 2002a, 2002b) shows a similar range of summit topography variations for the small shield volcanoes. It is expected that the terrestrial results will help us understand the contributions of local water availability and compositional evolution to topography in the ESRP. It should also have direct applicability to constraining similar questions on the chemical evolution and local water availability for our analogous martian plains volcanism regimes.

These results were presented in a set of paired sessions at the 2002 Fall Geological Society of America meeting in Denver in the session T90. Terrestrial Approaches to Extraterrestrial Problems and Vice Versa. (Sakimoto et al., 2002b, Hughes et al., 2002b).

References:

Hughes, S. S., M. McCurry, et al.. Geochemical correlations and implications for the magmatic evolution of basalt flow groups at the INEEL. Geology, Hydrogeology and Environmental Remediation, Idaho National Engineering and Environmental Laboratory. P. K. Link and L. L. Mink, Geol. Soc. of Am. Special Paper 353, 2002a.

Hughes, S.S., S.E.H. Sakimoto, and T.K.P. Gregg,Plains volcanism in the Eastern Snake River Plain: Quantitative measurements of petrologic contributions to topography with comparisons to Mars, GSA Annual Meeting Abstracts, Paper #77-3, 2002b.

Hughes S.S., R.P. Smith, W.R. Hackett, and S.R. Anderson Mafic volcanism and environmental geology of the eastern Snake River Plain, in Hughes, S.S., and Thackray, G.D., eds., Guidebook to the Geology of Eastern Idaho: Idaho Museum of Natural History, p. 143-168, 1999.

Hughes S.S., P.H. Wetmore, and J.L. Casper Evolution of Quaternary tholeiitic basalt eruptive centers on the eastern Snake River Plain, Idaho, in Bonnichsen, B., White, C., and McCurry M., eds., Tectonic and magmatic evolution of the Snake River Plain volcanic province: Idaho Geological Survey Special Publication, 2000.

Sakimoto, S.E.H., J.B. Garvin, B.A. Bradley, M. Wong, and J.J. Frawley, Small martian north polar volcanoes: Topographic implications for eruption styles, LPSC XXXII, CDROM, abstract #1808, 2001.

Sakimoto, S.E.H., D. Mitchell, S.J. Reidel, and K. Taylor, Small Shield Volcanoes on Mars: Global Geometric Properties and Model Implications for Regional Variations in Eruptive Styles, LPSC XXXIII, CDROM, abstract #1717, 2002.

Sakimoto, S.E.H., S.S. Hughes, T.K.P. Gregg, Plains volcanism on Mars: Topographic data on shield and flow distributions and abundances, with new quantitative comparisons to the Snake River Plain Volcanic Provinces, GSA Annual Meeting Abstracts, Paper #77-2, 2002b.

Contact: Susan Sakimoto, sakimoto@core2.gsfc.nasa.gov

Planetary Geology and Geophysics

Buried Basins on Mars

MOLA data has revealed an abundance of Quasi-Circular Depressions (QCDs) on Mars which have little or no expression in image data. These are most likely buried impact basins, covered versions of the impacts exposed at the surface. An earlier study of more than 600 of these in the lowlands of Mars showed that the crust below the young, smooth plains was as old and likely older than the exposed cratered highlands (Frey et al., 2002). In a paper given at the 2002 Lunar and Planetary Science Conference, Herb Frey showed that these buried lowland basins constrain the lowlands in eastern Mars to have formed in the earliest part of the Early Noachian, the oldest period of martian history (Frey, H., 2002). Further, in at least this part of Mars, the lowlands formed as the result of a giant impact. Though first suggested by George McGill in 1989 to be a giant impact, the Utopia Basin was not universally accepted as a larger version of Hellas or Argyre until MOLA topography showed its full bowl-like shape. Like the rest of the lowlands of Mars, this area has a large number of buried basins superimposed on it (Figure 29). These were shown by H. Frey and co-workers to be of Early Noachian age, meaning the Utopia impact which must pre-date these smaller basins is even older. Since the impact produced the low topography characteristic of this region (and since that imprint has remained intact since the impact), the crustal dichotomy in eastern Mars must date from essentially the earliest part of recorded martian history. Processes other than impact appear to have had little role to play in at least this part of Mars.

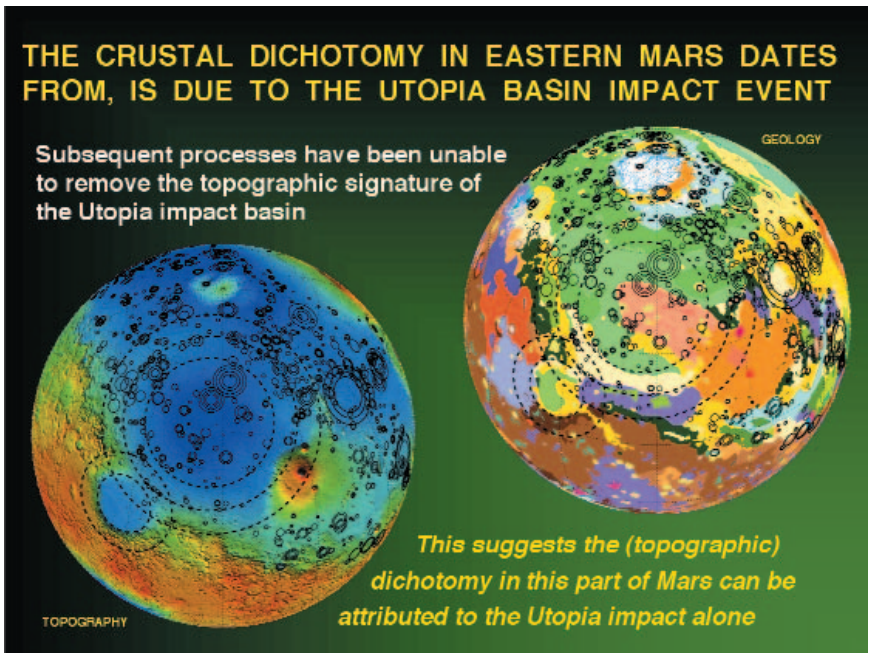

Figure 29. MOLA topography (lower left) and global geology (upper right) with lowland QCDs (mostly buried impact basins) superimposed on it. The large multi-ring structure is the Utopia impact basin, which is overlapped by the Isidis impact basin on its SW side. From Frey, H. 2002a.

Buried basins elsewhere on Mars have also provided evidence for crust older than the Early Noachian. In what started as a science fair project, sophomore Erin Frey of South River High School, working with her father, Herb Frey, found clear evidence for QCDs not visible on images in the oldest and most heavily cratered parts of Mars (Frey and Frey, 2002; Frey, E. et al., 2002). The region to the SE of the ancient Hellas impact basin, about 1.2 million sq km, is mapped as Early Noachian, based on its rugged nature and high density of craters. E. Frey found that there

was a significant population of buried basins in this area, which implies a crust below that is older than the surface. The total cumulative crater density is about 1.6 times that of the visible crater density. These results were presented at the Spring AGU Meeting in Washington by E. Frey (Frey and Frey, 2002) in her first professional paper. H. Frey did a similar study in the other major outcrop of Early Noachian terrain near the slightly younger (but still Early Noachian-age) Isidis impact basin and found similar evidence for an even larger population of buried basins (Frey, E. et al., 2002). Thus it appears what is mapped as Early Noachian material is not primordial crust on Mars dating back to 4.6 billion years ago. Curiously, in both the Hellas and Isidis areas the total crater density, the buried and visible populations together, are nearly the same. They are also very similar to the total crater density for several other Noachian areas (Figure 30).

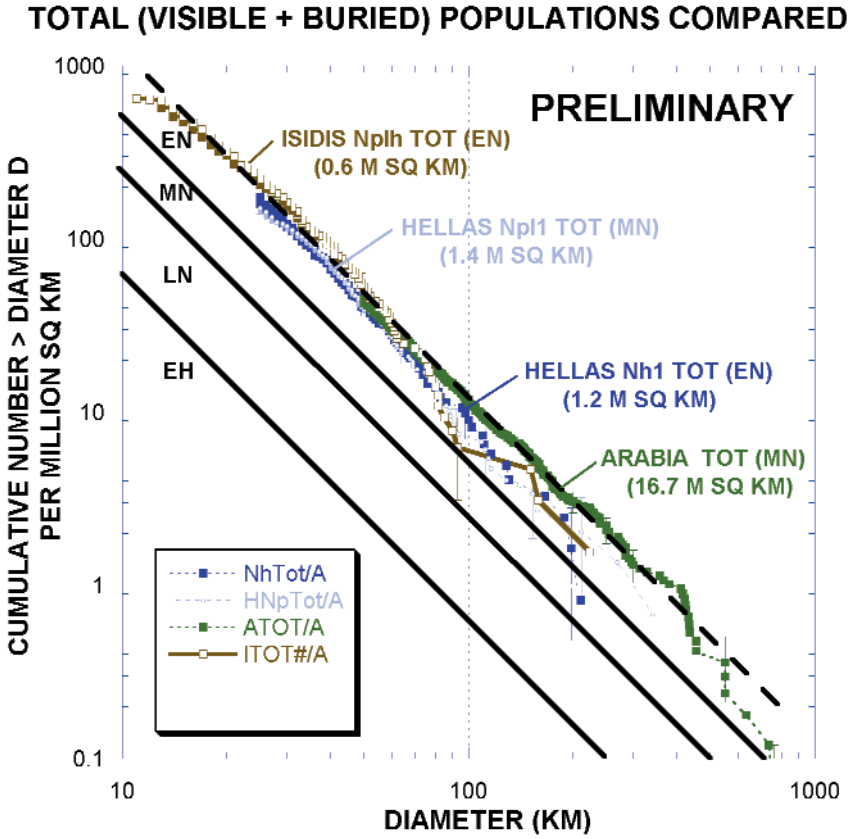

Figure 30. Total (visible + buried) cumulative frequency curves for several Noachian terrains, including a large area in Arabia and areas near the Hellas and Isidis impact basins. Note that all of these seem to show a similar crater retention age. From Frey, E. et al., 2002.

Similar total (visible + buried) crater retention ages for a number of different old units at different places around Mars could be due to crater saturation and might be a limit beyond which we cannot see and cannot date (in terms of impact craters) the buried surfaces. Alternatively, the similar crater retention age could represent a common early crustal age, perhaps of the original crust on Mars.

This work was presented at the Geological Society of America Meeting in Denver, CO (Frey, E., et al., 2002).

References:

Frey, E. L. and H. V. Frey, Evidence for an Earlier Early Noachian on Mars, Spring AGU Paper P32A-01, 2002.

Frey, E.L., H. V. Frey, W. K. Hartmann and K. L. Tanaka, Evidence for Crust Older than the Oldest Surface Units on Mars, GSA Annual Fall Meeting, Paper 26-2, 2002.

Frey H.V. Age and Origin of the Crustal Dichotomy in Eastern Mars, Lunar Planet Sci. Conf. XXXIII, abstract 1680, 2002.

Frey, H.V., J. H. Roark, K. M. Shockey, E. L. Frey and S. E. H. Sakimoto, Ancient Lowlands on Mars, Geophys. Res. Lett. 29, 10.1029/2001GL013832, 2002.

Contact: Herb Frey, Herbert.V.Frey@nasa.gov

Recent Studies of Mars Magnetic Anomalies

Why are some Martian terranes strongly magnetic and some non-magnetic? In a talk at the 33rd Lunar and Planetary Science Conference, Mike Purucker discussed the origin of a terrane, centered at Noachis Terra in the southern highlands, that has no strong magnitude magnetic fields (anomaoies) associated with it, unlike that of nearby terranes. This is enigmatic because the age of the rocks at the surface in the non-magnetic region is not much different from those in the adjacent, strongly magnetic region. Parts of this non-magnetic region are associated with the Argyre and Hellas impact basins, but one or more additional large impacts or thermal events may be necessary to produce such a region absent large-scale fields. Some candidates were suggested based on MOLA topographic data, which is useful for revealing even subtle depressions or basins.

As part of a popular presentation to a technical audience of non-specialists at the Society of Exploration Geophysicists, Purucker reviewed the state of knowledge on possible mineral resources on Mars. In a presentation called “Exploration Geophysics on Mars: A tale of Minerals and Water,” he also suggested the presence of deep concentrations of iron in the Terra Cimmeria and Sirenum regions, and the possible presence of near-surface Cu-Fe sulfides in the Apollinaris Patera region. An online version of the talk is available online at: http://geodynamics.gsfc.nasa.gov/research/purucker/mag_gravity_luncheon.html and a version is being prepared for publication in 'The Leading Edge.'

Contact: Mike Purucker, purucker@geomag.gsfc.nasa.gov

Atmospheric Rotational Effects on Mars Based on the NASA Ames General Circulation Model

The objective of this investigation is to compute and analyze how the atmosphere affects the rotation of Mars, based on outputs from the NASA Ames General Circulation Model (GCM). The model provides surface values of stress and pressure, which serve as inputs to the calculation of topographic (mountain), stress (friction), and gravitational atmospheric torques. The model also provides time series for the moments of inertia of the ice caps due to the condensation and sublimation of CO_2, and a time series for the axial component of atmospheric angular momentum.

The rotational variations of a planet can be analyzed into axial and equatorial components. The axial variations (along the z-axis, which is the rotation axis) are reflected in changes in the length of day (LOD). The equatorial variations (x,y) produce changes in the orientation of the axis of rotation (polar motion). The methodology of planetary rotational investigations can follow the angular momentum approach or the torque approach. The chosen methodology determines the boundaries of the appropriate control volume.

This investigation uses the torque approach to compute axial and equatorial variations in rotation. In this case the control volume includes only the solid body of Mars. The time variable moments of inertia produced by CO_2 condensation and sublimation are taken into account in the axial computations.

The angular momentum approach is used as well to obtain axial variations. The control volume then includes Mars' solid body and its atmosphere. Torques do not appear in this formulation.

Although experience with the Earth system indicates that the angular momentum approach is more reliable to compute LOD variations, the torque approach gives more insight on the mechanisms by which angular momentum is being transferred between the solid body and the atmosphere. Also, pressure and gravitational torques computed are not just the frictional component. Torque results are of interest on their own to ascertain the relative importance of various modes of angular momentum transfer.

In Mars' case the stress torque is the major contributor to the torque budget. This is different from the results obtained from Earth atmospheric models, in which case the ellipsoidal torques (polar flattening, gravitational) have by far the greatest total power magnitude, with the topographic torque ranking third.

The dominance of the frictional stress torque in Mars' budget can be attributed at least in part to the tangential stress dependency on the second power of the surface wind speeds. That is, Mars' less massive atmosphere (by a factor of 50) and the square of the wind speeds combine to produce smaller frictional stresses by a factor of 30, while Mars pressure torques are directly proportional to surface pressures which are 145 times smaller than Earth's. The solution of Liouville's equations provides the changes in Mars' rotation, i.e., changes in LOD and polar motion.

As shown in Figure 31, the polar motion computed from the torque forcing function reaches a maximum of 16.26 mm in the second half of the Martian Northern Hemisphere winter. The rotation pole moves around the axis of figure close to 3 and 1/2 times during the Martian year. Torque-induced annual and semi-annual polar motion is much less than the 21-cm obtained by other investigations from products of inertia due to ice caps offsets.

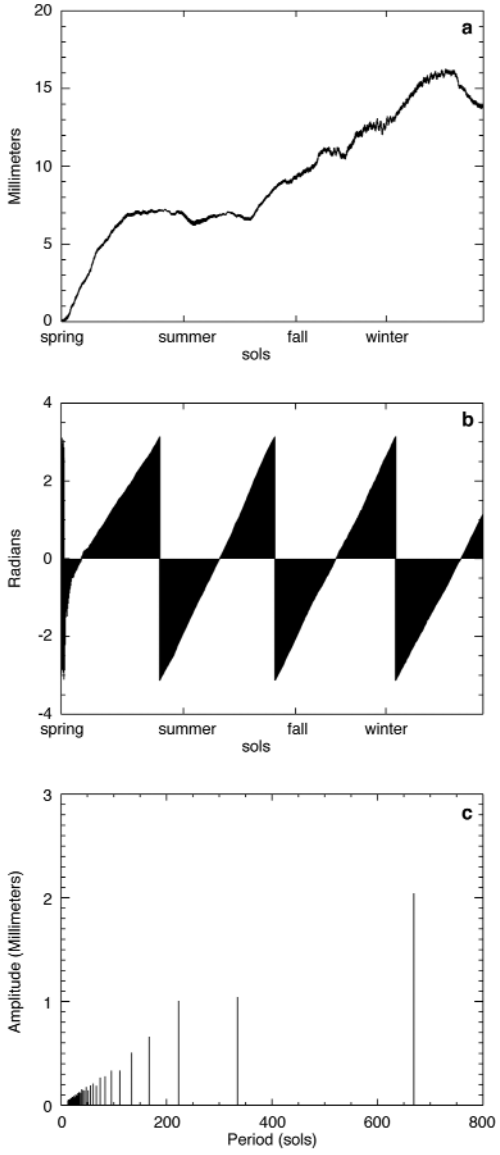

Figure 31. Polar motion due to torque, a) displacement time series, b) phase angle time series, c) displacement power spectrum.

Changes in LOD using the angular momentum approach are 0.187 and 0.136 milliseconds for the annual and semi-annual harmonics. The time series is portrayed in Figure 32. The expected precision of the planned NetLander Ionospheric and Geodesic Experiment (NEIGE) should detect

the main harmonics in the ΔLOD time series. Annual and semi-annual polar motion harmonics induced by atmospheric torque are below the level of NetLander Ionospheric and Geodesic Experiment (NEIGE) detectability. The model used here for the solid body of Mars does not include a liquid core; therefore possible near-diurnal resonances are excluded. We hope to study them in a future work.

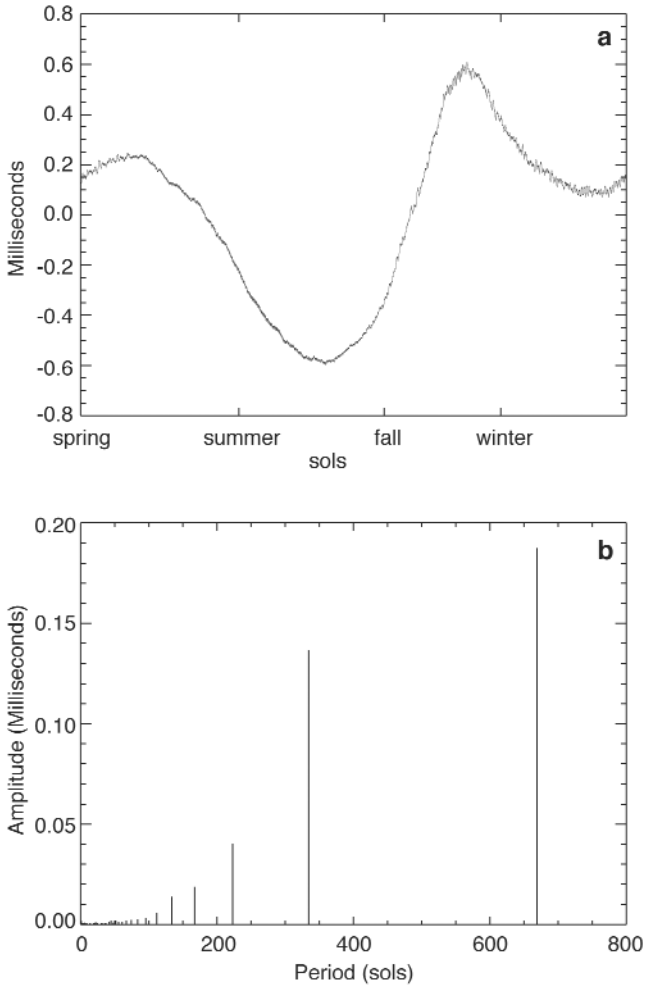

Figure 32. Delta LOD based on sum of axial atmospheric angular momentum and caps' inertia, a) time series, b) power spectrum.

Reference:

Sanchez, B. V., D. D. Rowlands, R. M. Haberle, J. Schaeffer, "Atmospheric Rotational Effects on Mars Based on the NASA Ames General Circulation Model", Journal of Geophysical Research - Planets, accepted January 16, 2003.

Contact: Braulio V. Sanchez, Braulio.V.Sanchez@nasa.gov

Orbital-Rotational-Climatic Interaction

Orbital Noise and Climate Fluctuation

The current debate on the Earth's climate fluctuations, (such as global warming) is driven by the observation of atmospheric concentrations of the greenhouse gases (CO_2 and CH_4). Popular climate models contain high levels of atmospheric carbon dioxide and predict that global greenhouse warming would cause heating in the tropics, but historical fossil isotopic data have indicated cool tropical temperature during greenhouse episodes. This mismatch between observation data and the climate models, known as the cool-tropic paradox, implies that either the data are flawed or we understand very little about the climate models.

Han-Shou Liu and co-workers (Liu, et al., 2002) suggest, from a dynamics point of view, that the common cause of climate and greenhouse-gas fluctuations is the orbital noise in the Earth's system which is distinct from the commonly considered orbital signals in eccentricity and precession. This finding provides a link between orbital noise and climate fluctuations for climate studies. Figure 33 shows calculations of insolation pulsation induced by orbital noise of the Earth's changing obliquity.

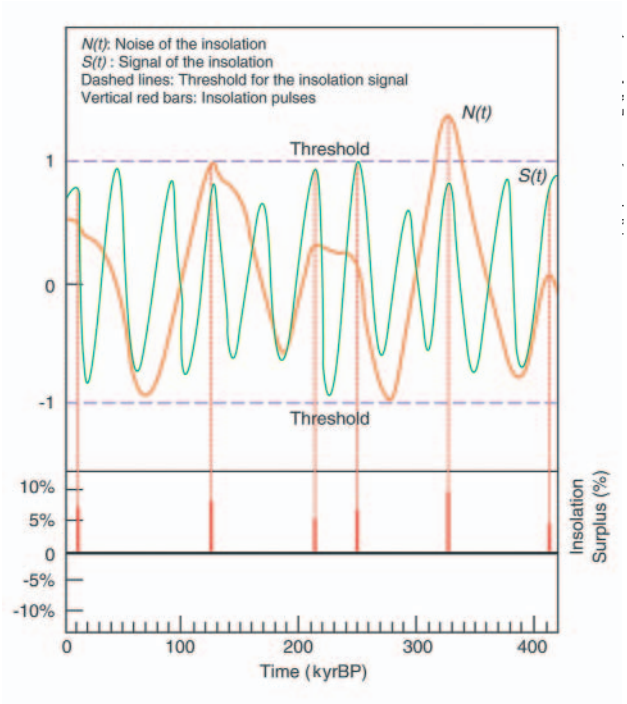

Figure 33. Noise-signal coupling effect on Rubincam's orbital insolation induces pulsation in the incoming solar radiation. The threshold model is derived from the signal to noise mode. The treshold (two horizontal dashed lines) defines the maximum and minimum values of the insolation signal. Time is in kiloyears (kyr) before present (BP).

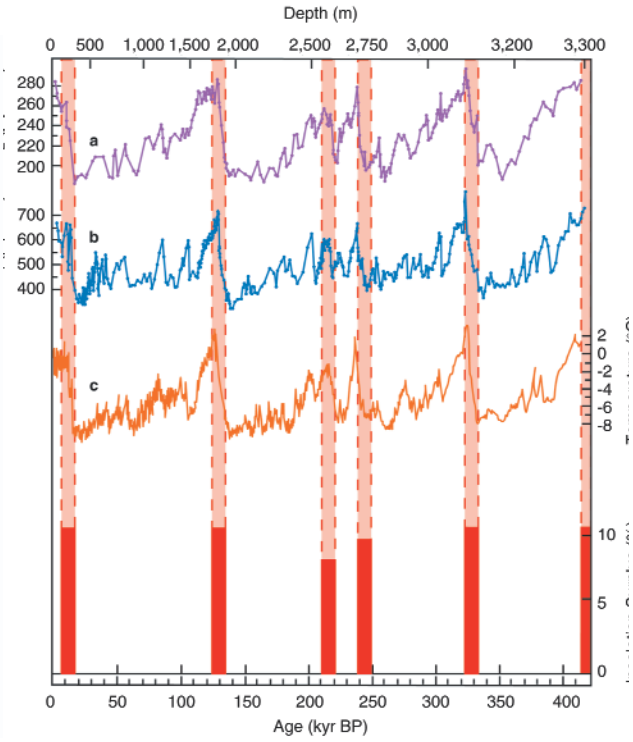

Figure 34. Orbital insolation pulses cause atmospheric concentrations of carbon dioxide and methane and glacial-interglacial temperature changes.

Global greenhouse warming phenomena during the past half million years were the effect and consequence of rapid temperature increases caused by insolation pulsation (Figure 34). In addition, Liu finds that the intensity of the insolation pulsation is dependent on the latitude of the Earth. At high latitude, it provides extreme climate warming conditions for greenhouse-gas concentration. However, it decreases markedly in low-latitude regions, predicting cool tropical temperature during supposed greenhouse episodes.

Reference:

Liu, H.S., R.Kolenkiewicz, and C. Wade, Orbital noise in the Earth system is a common cause of climate and greenhouse-gas fluctuation, Fluctuation and Noise Letters,Vol..2, No.2, 103-110, 2002.

Contact: Han Shou Liu,, Liu@core2.gsfc.nasa.gov

A Spin-Up for Asteroid 951 Gaspra

Gaspra, the first asteroid ever to be photographed up close by a spacecraft, is a small body only 6 km in radius, rotating with a 7 hour period, and orbiting in the asteroid belt at 2.2 AU from the Sun. Gaspra's axial precession period turns out to be nearly commensurate with its orbital precession period. This leads to a resonance condition with huge variations in obliquity (obliquity being the tilt of Gaspra's equator with respect to its orbital plane). How did the asteroid get into this resonance? One way is for the orbit to change over time. However, computing its orbit for the last 3 million years indicates its orbit is highly stable (see Figure 35).

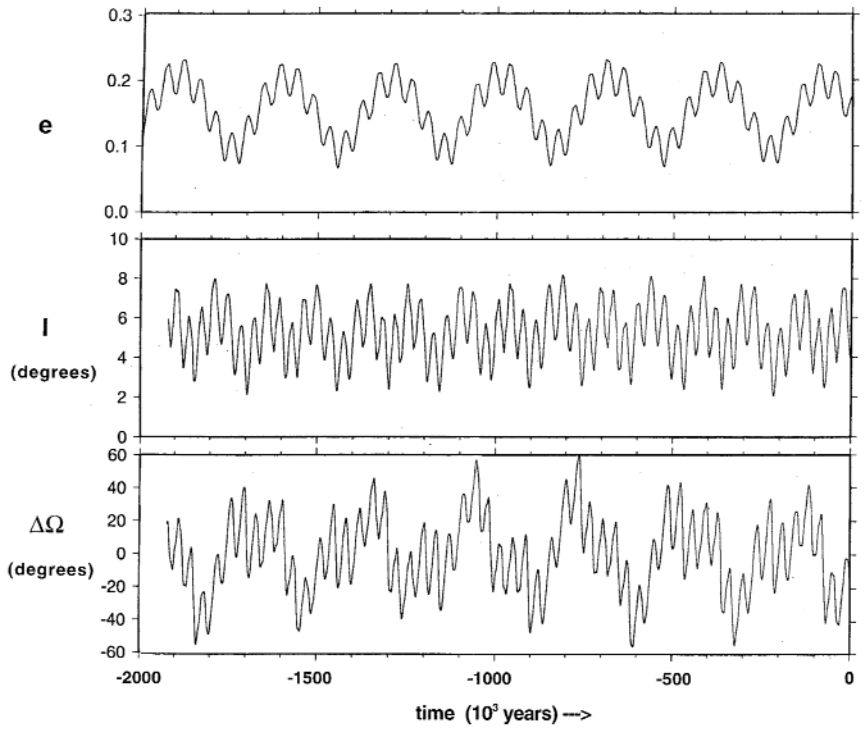

Figure 35. Evolution of the orbit of Gaspara over the last two million years.

A more likely explanation is the YORP effect (Rubincam et al., 2002). YORP stands for Yarkovsky-O'Keefe-Radzievskii-Paddack. In the YORP effect, Gaspra absorbs sunlight and re-

radiates it mostly as heat in the infrared. The infrared photons leaving the surface carry away momentum. By action-reaction, the asteroid receives a slight kick in the opposite direction. It is here the highly shape of Gaspara, known from photographs to be highly irregular, come into play. As shown in Figure 36, the re-radiation causes a net torque on the asteroid, making it spin faster. A change in the spin rate causes the obliquity to change.

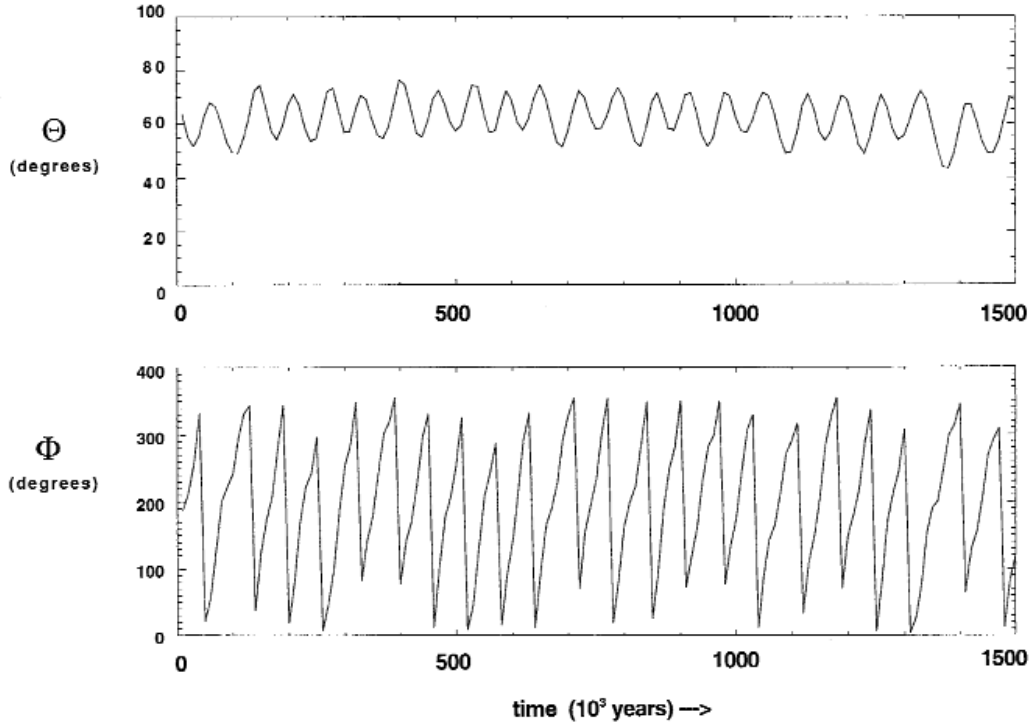

Figure 36. Change in spin and change in obliquity for Gaspra.

It may be that Gaspra started out in a nonresonant state, but evolved into the resonance due to the YORP effect, and has been temporarily trapped there ever since. YORP can alter the spin of small asteroids like Gaspra over hundreds of millions of years, making it competitive with collisions in this regard. Thus YORP may be a major mechanism for altering the spin states of small asteroids and meteorites. These results were published in the September 2002 issue of Journal of Geophysical Research: Planets.

References:

Rubincam, D. P., D. D. Rowlands, and R. D. Ray, Is asteroid 921 Gaspra in a resonant obliquity state with its spin increasing due to YORP?, J. Geophys. Res., 107, 5065, doi:10.1029/2001JE001813, 2002.

Contact: Dave Rubincam, David.P.Rubincam@nasa.gov

Refereed Journal Publications:

Beasely, A. J., **D. Gordon**, A. B. Peck, **L. Petrov**, **D. S. MacMillan**, E. B. Fomalont, and **C. Ma**, The VLBA calibrator survey—VCS1, *Astrophys. J. Sup. Ser.*, *141*, 13-21, 2002.

Cheng AF, Barnouin-Jha O, Prockter L, **Smith, DE**, et al., "Small-scale topography of 433 Eros from laser altimetry and imaging", ICARUS 155 (1): 51-74, 2002

Cohen, S.C. and D.J. Darby, Tectonic plate coupling and elastic thickness derived from the inversion of geodetic data using a steady-state viscoelastic model: Application to southern North Island, New Zealand, *J. Geophys. Res*., 2001JB01687, 2002.

Cox, C. M., and **B. F. Chao**, Detection of a large-scale mass redistribution in the terrestrial system since 1998, *Science*, *297*, 831-833, August 2, 2002.

Cox, C. M., S. M. Klosko, and **B. F. Chao,** Changes in ice-mass balances inferred from time variations of the geopotential observed through SLR and DORIS tracking, in gravity, geoid and geodynamics, M. Sideris ed., IAG Symposia 123, Springer-Verlag, Heidelberg, 2002.

Frey, H.V., J. H. Roark, K. M. Shockey, E. L. Frey and **S. E. H. Sakimoto**, Ancient Lowlands on Mars, *Geophys. Res. Lett*. 29, 10.1029/2001GL013832, 2002.

Fujita, M., **B. F. Chao, B. V. Sanchez**, and T. J. Johnson, Oceanic torques on solid Earth and their effects on Earth rotation, *J. Geophys. Res*., *107*, NO. B8, 10.1029/2001JB000339, 2002.

Heirtzler JR, "The future of the South Atlantic anomaly and implications for radiation damage in space", J ATMOS SOL-TERR PHY 64 (16): 1701-1708, 2002

Hulot G., C. Eymin, **B. Langlais**, M. Mandea, and N. Olsen, Small-scale structure of the geodynamo inferred from Ørsted and MAGSAT satellite data, *Nature*, 416, pp. 620-623, 2002.

Kim, H. R., R. R. B. von Frese, J. W. Kim, **P. T. Taylor** and T. Neubert, Ørsted verifies regional magnetic anomalies of the Antarctic lithosphere, *Geophysical Research Letters*, vol. 29, no. 15, p. 31-33, 2002.

Kletetschka, G., P. J. Wasilewski and **P. T. Taylor**, The role of hematite-limonite solid solution in the production of magnetic anomalies in ground- and satellite-based data, *Tectonophysics*, vol. 347 no. 1-2, p. 167-178, 2002

Kutina, J. and **P. T. Taylor**, Satellite altitude magnetic anomalies-implications for mineral exploration: A review, *Global Tectonics and Metallogeny*, vol. 8, no. 1-2, 2002.

Liu, H. S., R. Kolenkiewicz, and **C. Wade, Jr.,** Orbital noise in the Earth system is a common cause of climate and greenhouse-gas fluctuation, *Fluctuation and Noise Lett. 2,* L101-L108, 2002.

Lowman, P. D., "Exploring Space, Exploring Earth: New Understanding of the Earth from Space Research," Cambridge University Press, 362 p., 2002.

Lowman, P. D., "Exploration Science: A Case History from Earth Orbit," *The Science Teacher*, v. 69, no. 7, p. 24-30, 2002.

Luhmann, J.G., M.H. Acuna, **M. Purucker**, C.T. Russell, and J.G.Lyon, The Martian magnetosheath: how Venus-like?, *Planetary and Space Science*, 50, 489-502, 2002.

Luthcke, S. B., **C. C. Carabajal** and **D. D. Rowlands**, Enhanced geolocation of spaceborne laser altimeter surface returns: parameter calibration from the simultaneious reduction of altimeter range and navigation tracking data, *Journal of Geodynamics*, *34*, 447 – 475, 2002.

McGovern, P., S.C. Solomon, J.W. Head, **D.E. Smith, M.T. Zuber**, M. A. Wieczorek, R.J. Phillips, **G.A. Neumann**, O. Aharonson, Localized gravity/topography admittance and correlation spectra on Mars: Implications for regional and global evolution, *J. Geophys. R*es., 107(E12), 5136, DOI:10.1029/2002JE001854, 2002.

Mendes, V. B., G. Prates, **E. C. Pavlis**, **D. E. Pavlis**, and R. B. Langley "Improved mapping functions for atmospheric refraction correction in SLR", *Geophysical Res. Lett., 29*(10), 1414, doi:10.1029/2001GL014394, 2002.

Pavlis, E. C., "Geodetic Contributions to Gravitational Experiments in Space", Book chapter in *Recent Developments in General Relativity, Genoa 2000*, R. Cianci, R. Collina, M. Francaviglia, P. Fré (eds), Springer-Verlag, Milan, pp. 217-233, 2002.

Pavlis, E. C. and L. Iorio, "The impact of tidal errors on the determination of the Lense-Thirring effect from satellite laser ranging", *International Journal of Modern Physics D*, 11, 4, pp. 599-618, 2002.

Peale SJ, Phillips RJ, Solomon SC, **Smith DE**, et al., "A procedure for determining the nature of Mercury's core", METEORIT PLANET SCI 37 (9): 1269-1283 SEP 2002

Ponte, R. M. and **R. D. Ray**, `Atmospheric pressure corrections in geodesy and oceanography: a strategy for handling air tides,' *Geophysical Research Letters, 29(24),* 6.1-6.4, 2002.

Purucker, M., B. Langlais, N. Olsen, G. Hulot, and M. Mandea, The southern edge of cratonic North America: Evidence from new satellite magnetometer observations, *Geophys. Res. Lett*., 29, 1 August 2002.

Ravat, D., B. Wang, E. Wildermuth and **P. T. Taylor**, Gradients in the interpretation of satellite-altitude magnetic data: an example from central Africa, *Journal of Geodynamics*, vol. 33 no. 1-2, p.131-142, 2002.

Ravat, D., K. Whaler, M. Pilkington, **T. Sabaka and M. Purucker**, Compatibility of high-altitude aero-

magnetic and satellite-altitude magnetic anomalies over Canada, **Geophysics**, 67, 546-554, 2002

Rowlands, D. D,. R. D. Ray, D. S. Chinn and **F. G. Lemoine**, Short-arc analysis of intersatellite tracking data in a gravity mapping mission, *Journal of Geodesy, 76,* 307-316, 2002.

Rubincam, D. P., **D. D. Rowlands,** and **R. D. Ray**, Is asteroid 951 Gaspra in a resonant obliquity state with its spin increasing due to YORP? *Journal of Geophysical Research, 107,* 1-7, 2002.

Sabaka, T.J., N. Olsen and **R.A. Langel**, A comprehensive model of the quiet-time, near-Earth magnetic field: phase 3, *Geophys. J. Int*., 151, 32-68, 2002.

Taylor, P.T. and J.J. Frawley, Satellite-Altitude-Magnetic Data and the Search for Mineral Resources: the Kiruna region of Sweden, *Global Tectonics and Metallogeny*, vol. 8, no. 1-2, 2002

Voorhies, C.V., T.J. Sabaka, and M. Purucker, On magnetic spectra of Earth and Mars, *J. Geophys. Res*., 10.1029/2001/JE001534, 04 June 2002.

Withers, P., R. D. Lorenz and **G. A. Neumann**, Comparison of Viking Lander descent data and MOLA topography reveals kilometer-scale offset in Mars atmosphere profiles, *Icarus,* 159, 259–261, doi:10.1006/icar.2002.6914, 2002.

Zweck, C., J. T. Freymueller, and **S .C. Cohen**, Three dimensional elastic dislocation modeling of the postseismic response to the 1964 Alaska Earthquake, *J. Geophys. Res*., 107(B4), 10.1029/2001JB00409, 2002.

Zweck, C., J. T. Freymueller, and **S. C. Cohen**, The 1964 Great Alaska Earthquake; Present day and cumulative postseismic deformation in the western Kenai Peninsula, *Phys. Earth Planet. Int*., 132, 5-20, 2002.

Conference Proceedings Papers:

Colombo, O. L., **S. B. Luthcke**, **D. D. Rowlands**, **D. Chin** and **S. Polouse**, Filtering errors in LEO trajectories obtained by kinematic GPS with floated ambiguities, *Institute of Navigation International Symposium "GPS 2002"*, Portland, Oregon, September 24-27, 2002.

MacMillan, D. S., L. Petrov, and C. Ma,, Geodetic results from Mark4 VLBI, *IVS General Meeting Proceedings*, 50-54, February 4-7, 2002.

Ma C., D. S. MacMillan, and L. Petrov, Integrating analysis goals for EOP, CRF, and TRF, *IVS General Meeting Proceedings*, 255-259, February 4-7, 2002.

Ma C., D. Gordon, D. S. MacMillan, and L. Petrov, Towards a future ICRF realization , *IVS General Meeting Proceedings*, 355-359, February 4-7, 2002.

Mertikas, S., **E. C. Pavlis**, Th. Papadopoulos, and X. Frantzis Preparatory steps for the establishment of a European radar altimeter calibration and sea-level monitoring site for JASON, ENVISAT and EURO-GLOSS, in Proceedings of the *2001 IAG Scientific Assembly: Vistas for Geodesy in the New Millennium*, of the *International Association of Geodesy*, Budapest, Hungary, September 2-7, 2001, electronic publication (CD), 2002.

Pavlis, E. C. Dynamical determination of origin and scale in the Earth system from satellite laser ranging, in *Vistas for Geodesy in the New Millennium*, proceedings of the 2001 International Association of Geodesy Scientific Assembly, Budapest, Hungary, September 2-7, 2001, J. Adam and K.-P. Schwarz (eds.), Springer-Verlag, New York, pp. 36-41, 2002.

Purucker, M., H. McCreadie, S. Vennerstroem, G. Hulot, N. Olsen, H.Luehr, and E. Garnero, Highlights from AGU's Virtual Session on New Magnetic Field Satellites, *EOS*, 83, 368, August 20, 2002 (with associated CD-ROM).